Supporting Information

Table of Contents

Scheme S1: Synthesis of the precursor **1**.

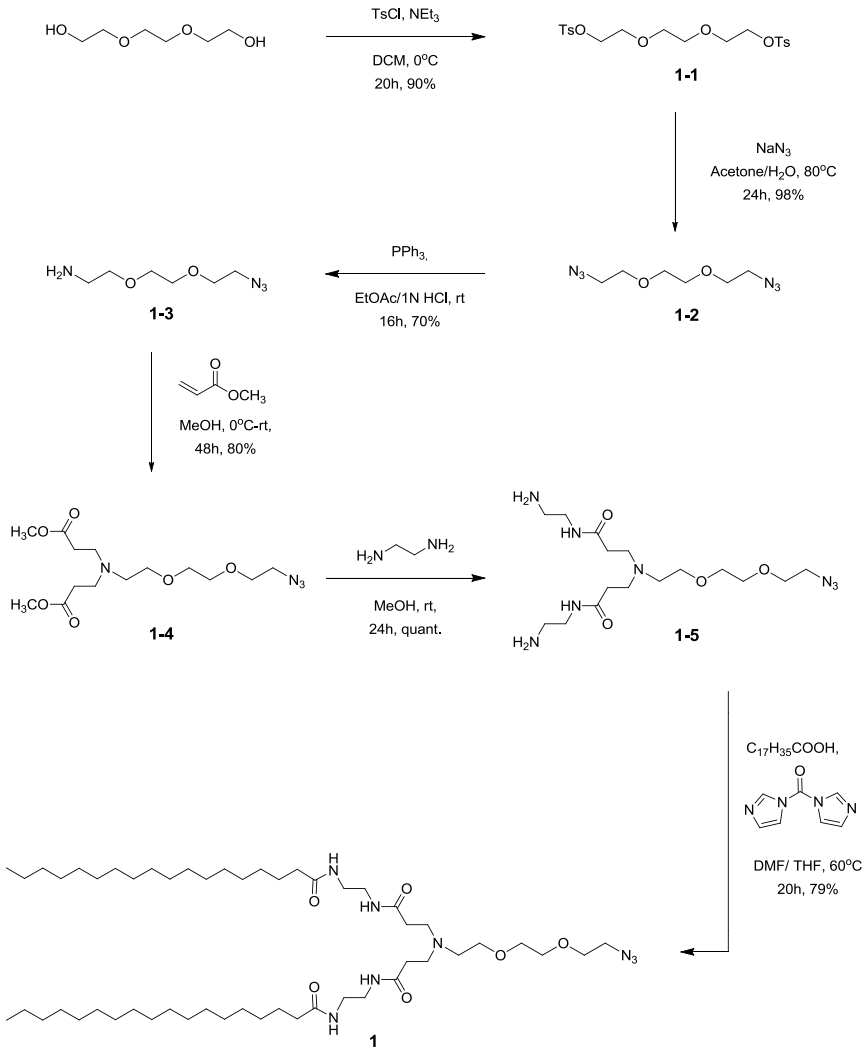

Scheme S2: Synthesis of the precursor **2**.

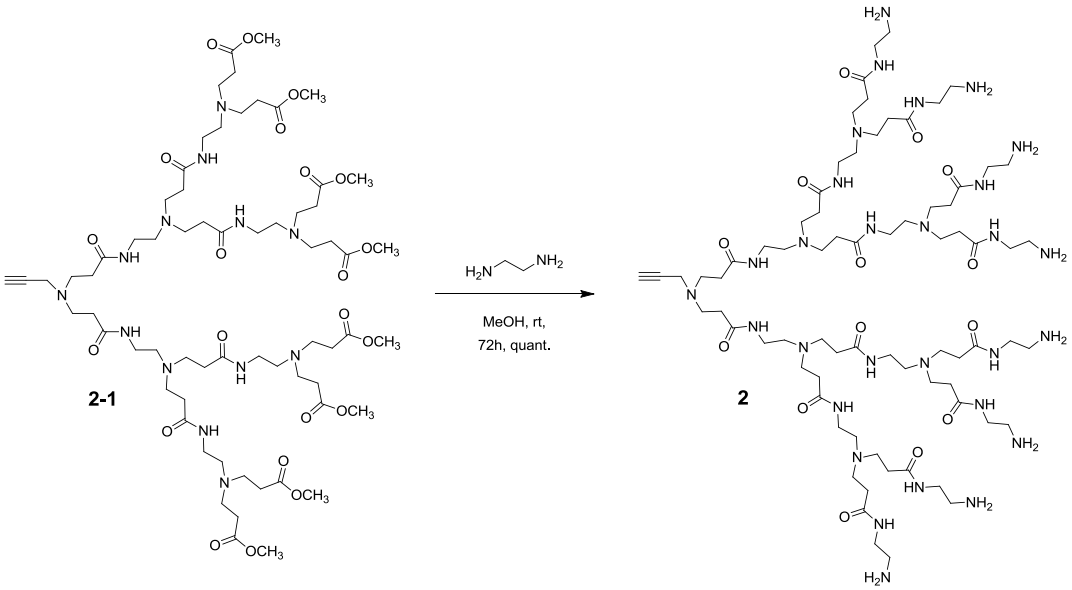

Scheme S3: Synthesis of the amphiphilic dendrimer **AD**.

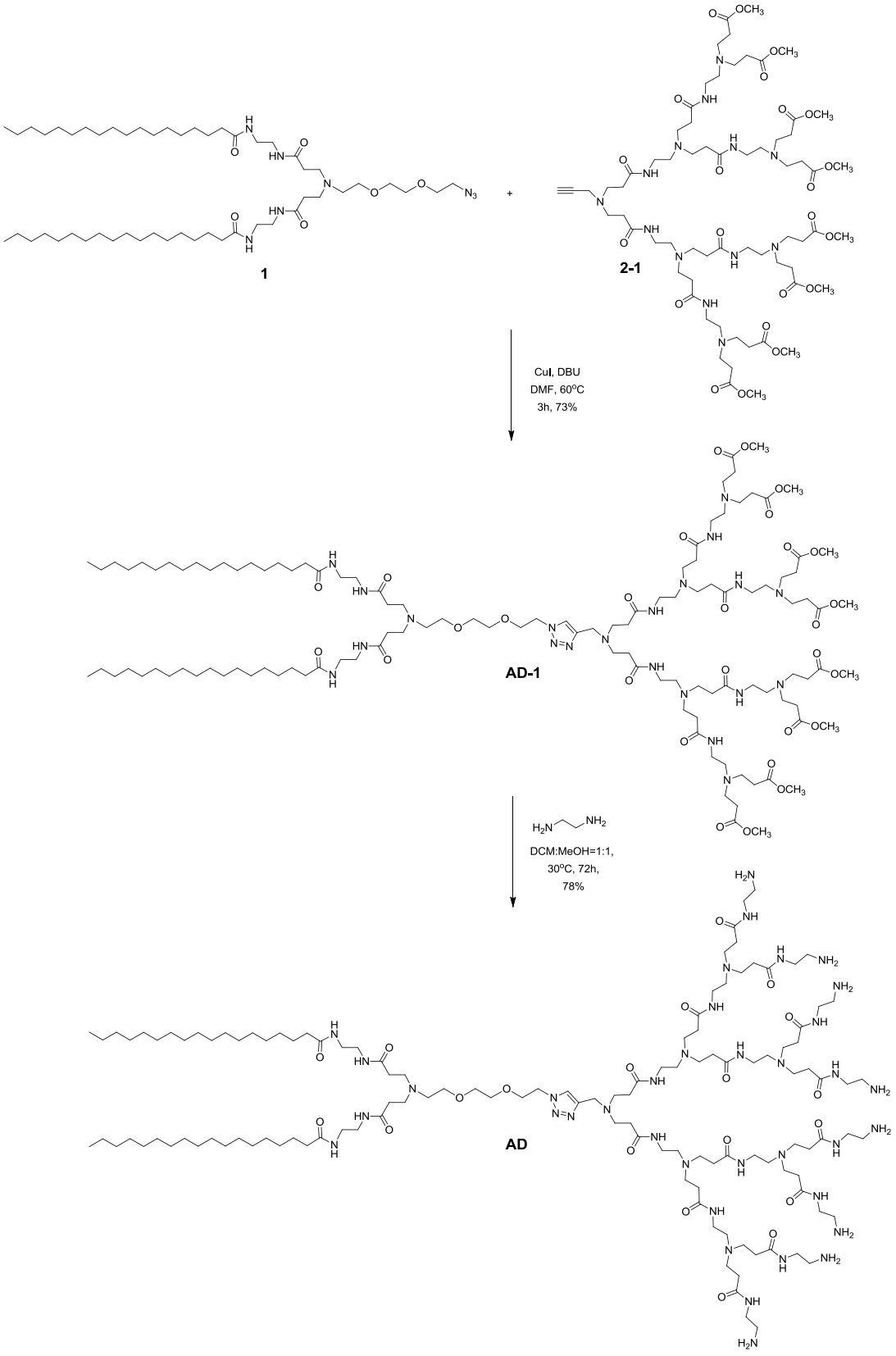

Figure S1: Self-assembly studies of the amphiphilic dendrimer **AD**. (**A**) Pressure – Area isotherm of a monolayer of **AD** at water/air interface recorded using a Langmuir film-balance equipped with a Wilhelmy plate as pressure sensor. The area is expressed as the total area of the film as it is compressed. (**B**) Giant vesicles formed in sucrose solution using electro-swelling method. (**C**) The critical micelle concentration (CMC) of dendrimer **AD** measured using the fluorescent dye pyrene.

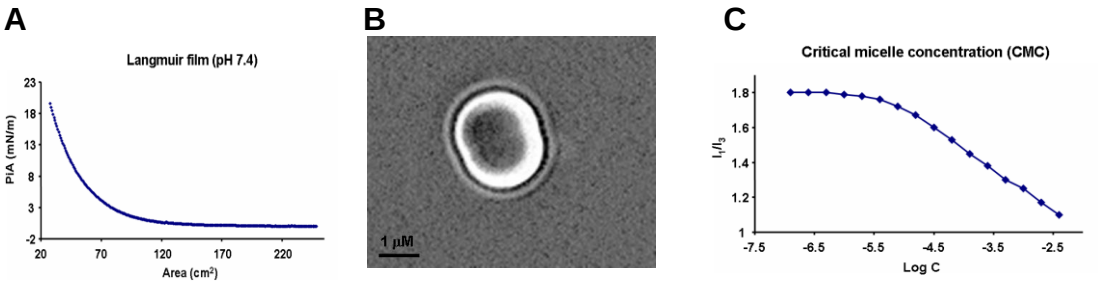

Figure S2: Potentiometric pH back titration of the completely protonated form of the amphiphilic dendrimer **AD**.

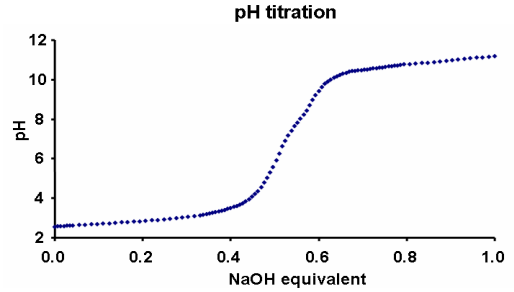

Figure S3: Binding of siRNA and **AD** was measured using fluorescent titration of ethidium bromide (25.4 μM) in complex with siRNA (20 μM per base pair) by **AD** in phosphate buffered saline (PBS) at pH=7.4. The normalized fluorescence intensity decreased with increasing concentration of **AD** since ethidium bromide was displaced from the siRNA/**AD** complexes upon addition of **AD**.

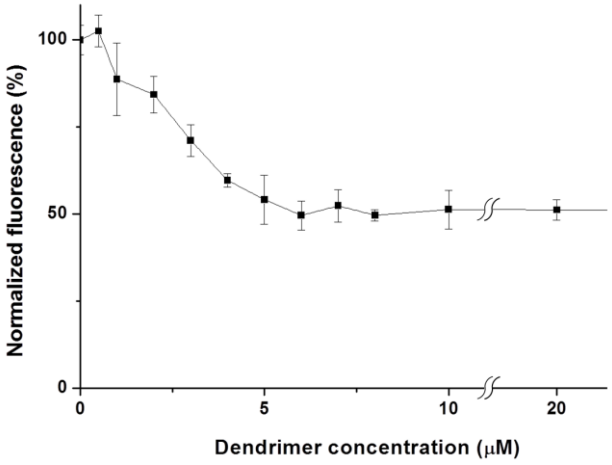

Figure S4: The hallmark of macropinocytosis - actin rearrangement in PC-3 cells in presence of siRNA/dendrimer **AD** complexes (20 nM Hsp27 siRNA and **AD** at a N/P ratio of 10) was tracked by confocal microscopy using Alexa647-labeled phalloidin fluorescent probe. DAPI was used to label the nuclei.

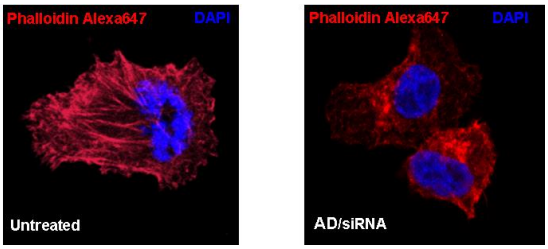

Figure S5: The amphiphilic dendrimer **AD** mediated siRNA delivery and gene silencing in adherent breast cancer MDA-MB231 and MCF-7 cells, suspended human mantle cell lymphoma (MCL) (Jeko-1 cells) and human glioblastoma stem cells: (**A**) human breast cancer MDA-MB231 cells treated with 50 nM Hsp27 siRNA and **AD** at a N/P ratio of 10; (**B**) human breast cancer MCF-7 cells treated with 20 nM Hsp27 siRNA and **AD** at a N/P ratio of 10, (**C**) human mantle cell lymphoma (MCL) (Jeko-1 cells) and (D) human glioblastoma stem cells (PBT003 cells) treated with 50 nM dsiRNA targeting signal transducer and activator of transcription 3 (STAT3) and **AD** at a N/P ratio of 5. *, **, ***, and ****, differ from control ($p \leqslant 0.05$, $p \leqslant 0.01$, $p \leqslant 0.001$, and $p \leqslant 0.0001$, respectively) by Student's *t* test.

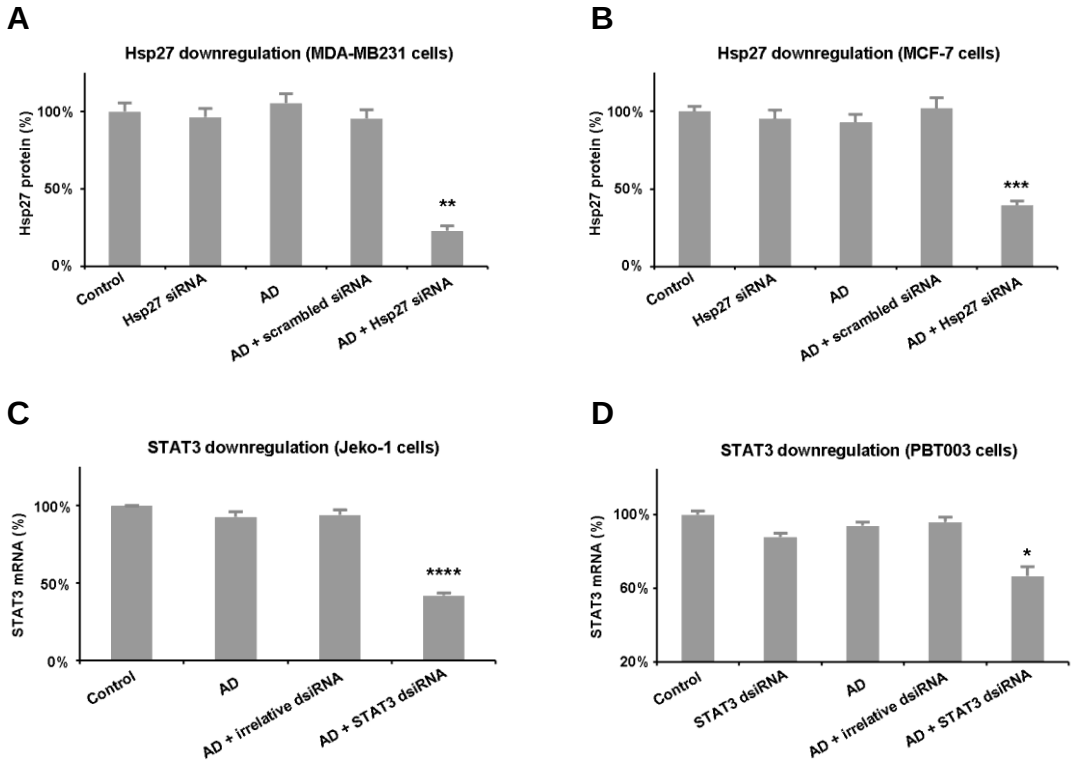

Figure S6: No discernible toxicity was observed in different cells following treatment with the siRNA/**AD** complexes. Toxicity on prostate PC-3 cells was assessed using (**A**) LDH and (**B**) MTT assay after treatment with 20 nM siRNA and **AD** at a N/P ratio of 10. The toxicity profile on (**C**) CEM T-cells, (**D**) PBMC CD4+ cells, (**E**) CD34+ stem cells and (**F**) human glioblastoma stem cells (PBT003 cells) was measured using MTS assay following treatment with 50 nM dsiRNA and **AD** at a N/P ratio of 5.

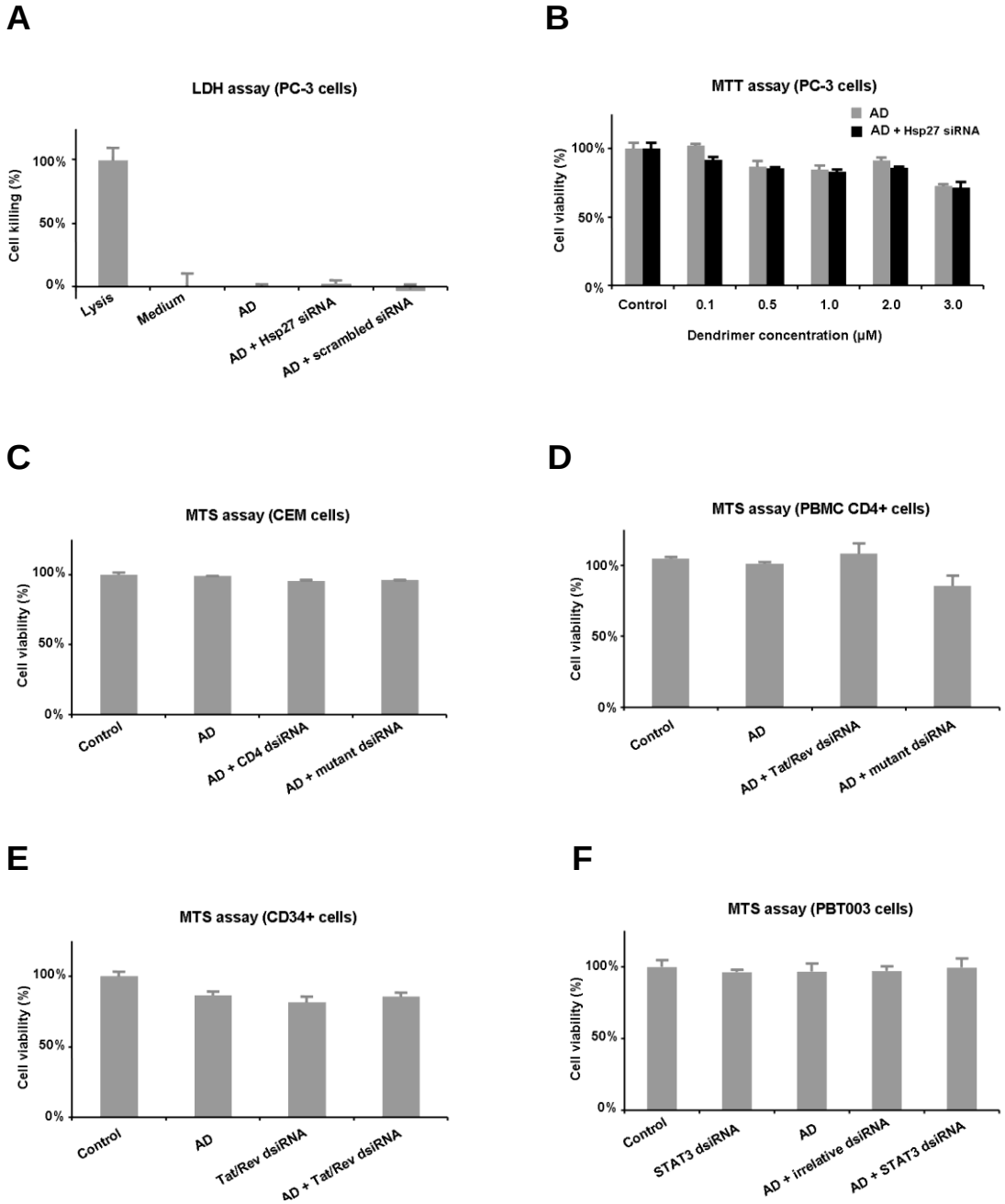

Figure S7: The amphiphilic dendrimer **AD** mediated siRNA delivery and gene silencing of Hsp27 in prostate cancer PC-3 cells could be maintained (**A**) over one week following treatment with 20 nM siRNA and **AD** at a N/P ratio of 10, as well as (**B**) in medium containing 10% serum in the presence of chloroquine (50 μM) at N/P ratios of 10 and 20. ** and ***, differ from control ($p \leqslant 0.01$, $p \leqslant 0.001$, respectively) by Student's *t* test.

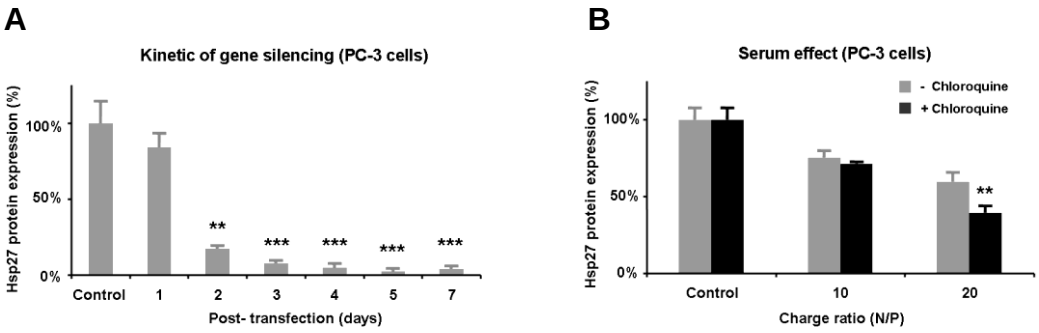

Figure S8: Significant inhibition of cell proliferation via caspase dpendent apoptosis induction following the amphiphilic dendrimer **AD** mediated siRNA delivery and gene silencing of Hsp27 in prostate cancer PC-3 cells with 20 nM siRNA and **AD** at an N/P ratio of 10. Cell proliferation was assessed by (**A**) MTT assay and (**B**) crystal violet assay 6 days post-treatment. (**C**) Caspase-3/7 activation was evaluated using a colorimetric assay 2 days post-treatment. (**D**) Apoptotic cells were quantified with FACS flow cytometry using Annexin V staining 3 days post-treatment. **, differ from control ($p \leqslant 0.01$) by Student's *t* test.

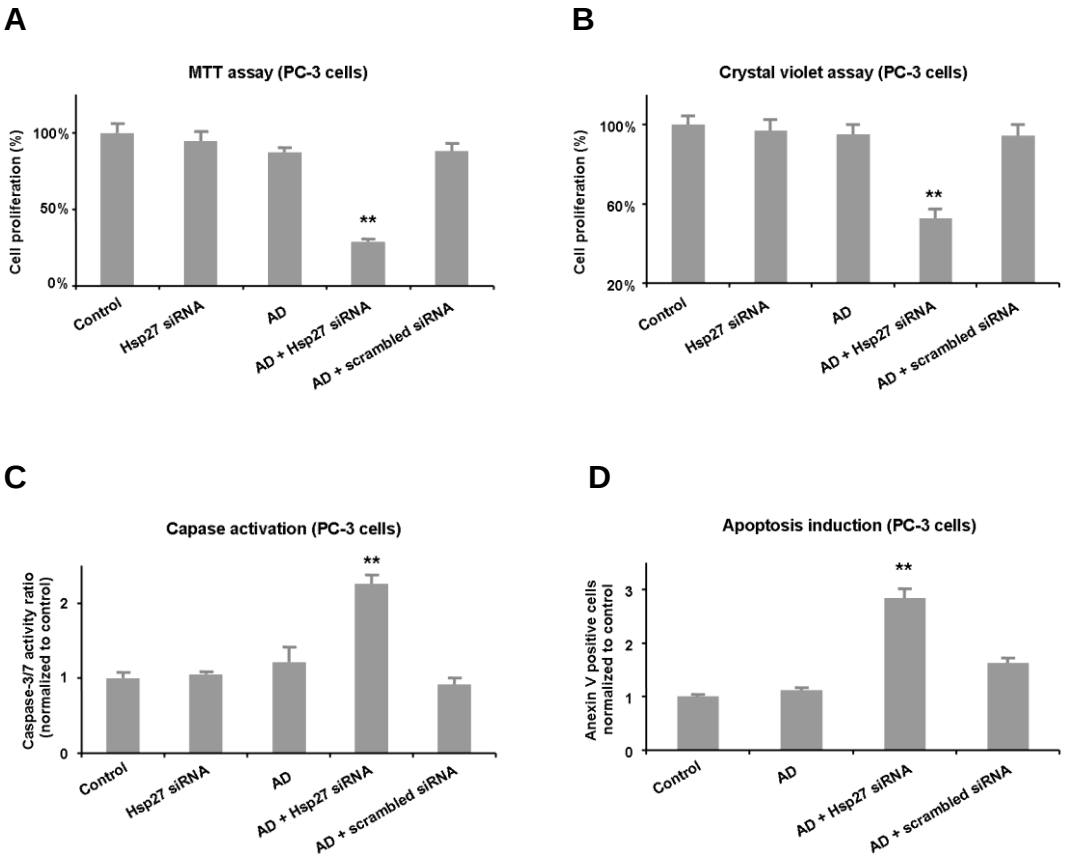

Figure S9: Effective inhibition of HIV replication in (**A**) primary human peripheral blood mononuclear cells (PBMC-CD4+ cells) and (**B**) hematopoietic stem cells CD34+ (Figure 3F) following treatment with the anti-*tat/rev* dsiRNA delivered by **AD** with 50 nM dsiRNA and **AD** at a N/P ratio of 5. Viral loading was assessed using HIV-1 p24 antigen ELISA at 3 days of post-treatment. PBMC CD4+ cells and CD34+ cells were infected by NL4-3 virus (MOI 0.001) and JR-FL virus (MOI 0.005) respectively for 5 days before transfection. * and ***, differ from control ($p \leq 0.05$ and $p \leq 0.001$, respectively) by Student's *t* test.

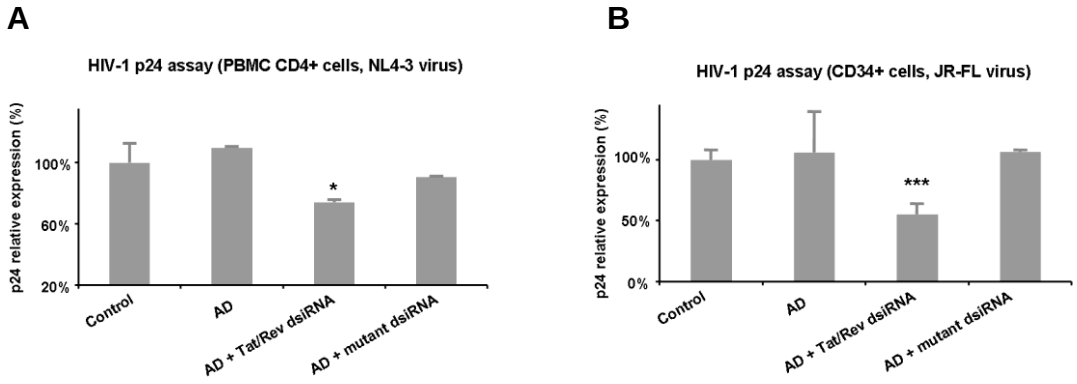

Figure S10: Commercial transfection reagent Lipofectamine RNAiMAX (lipo) was not able to effectively mediate gene silencing in (**A**) primary PBMC CD4+ cells nor (**B**) CD34+ stem cells using CD4 dsiRNA (50 nM), nor (**C**) human glioblastoma stem cells (PBT003 cells) using STAT3 dsiRNA (50 nM) following the protocols of the manufacture.

A

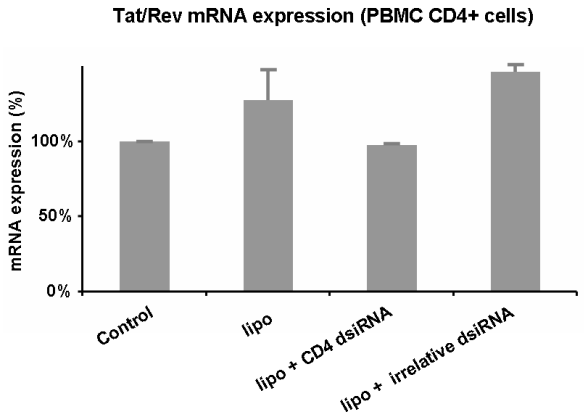

B

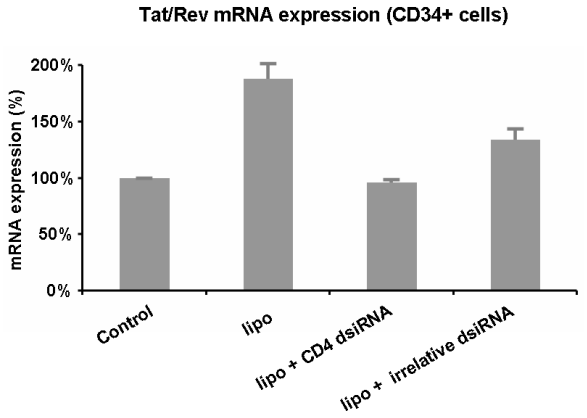

C

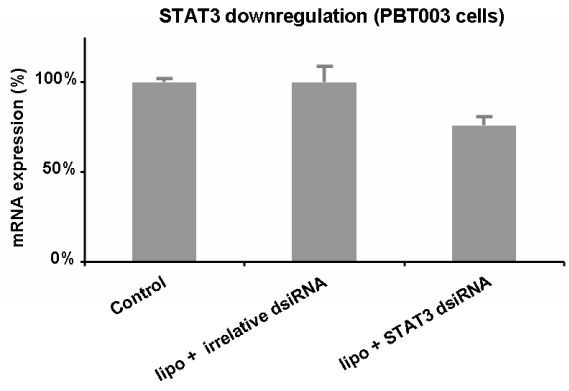

Figure S11: No weight alteration for the prostate cancer PC-3 tumor xenografted nude mice treated with intraperitoneal administration of the siRNA/**AD** complexes, PBS buffer, siRNA alone, **AD** alone and scramble siRNA/**AD** complexes (3 mg/kg Hsp27 siRNA and **AD** at N/P ratio of 5) during a period of 5 weeks with an injection frequency of twice a week.

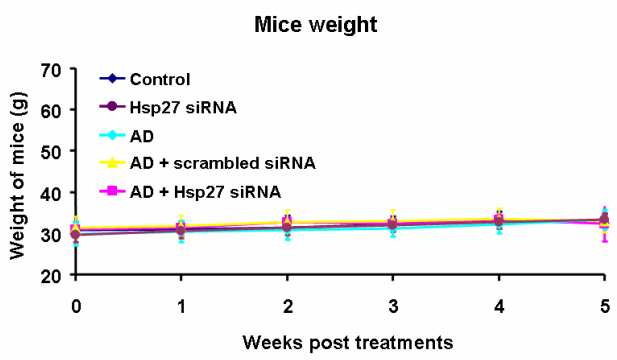

Figure S12: No pathology and dysfunction were revealed in the major organs of the male C57BL/6 mice treated with intravenous administration of siRNA/**AD** (3 mg/kg siRNA and **AD** at a N/P ratio of 5), compared with the non-treatment, naked siRNA alone, **AD** alone respectively. (**A**) Sectioning and staining the major mouse organs including heart, kidney, liver, lung, and spleen with H&E after mice being sacrificed 24 hours post-treatments. Organs function was examined by (**B**) measuring the hepatic enzyme level with the indicators of alanine transferase (ALT) and gamma glutamyl transferase (γ-GT), (**C**) monitoring the kidney function with the indicators of creatinine (CRE) and blood urea nitrogen (BUN), and (**D**) recording the cholesterol (CHO) level in the blood.

A

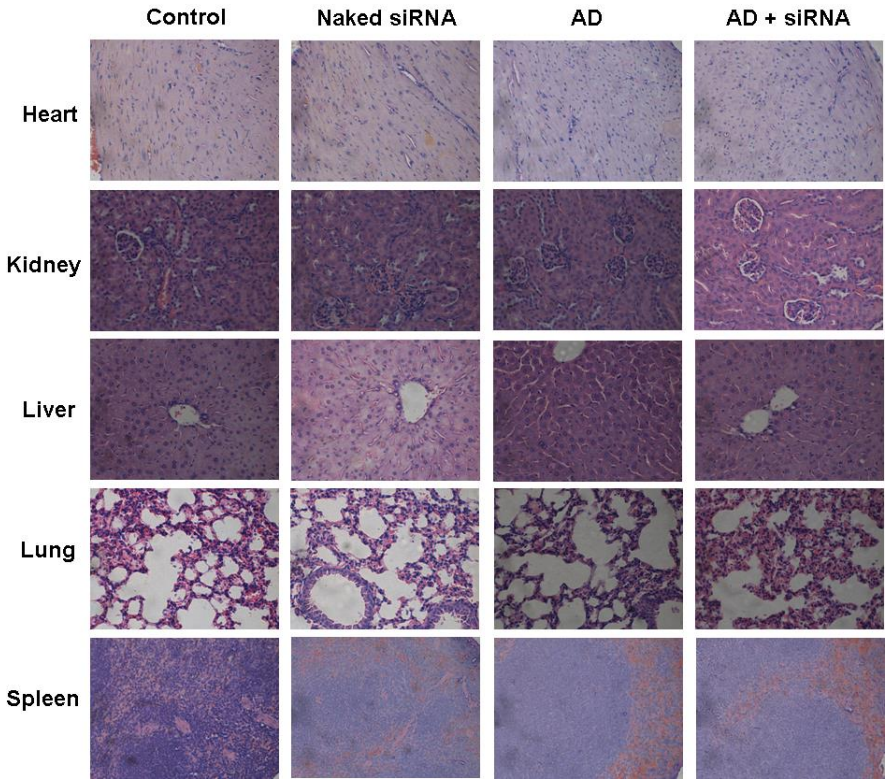

B

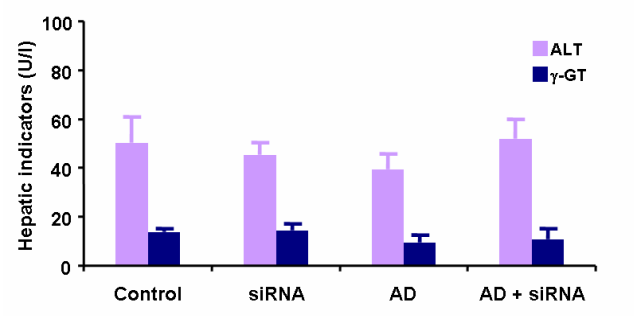
Hepatic indicators (U/l)
100
80
60
40
20
0
ALT
γ-GT
Control
siRNA
AD
AD + siRNA

C

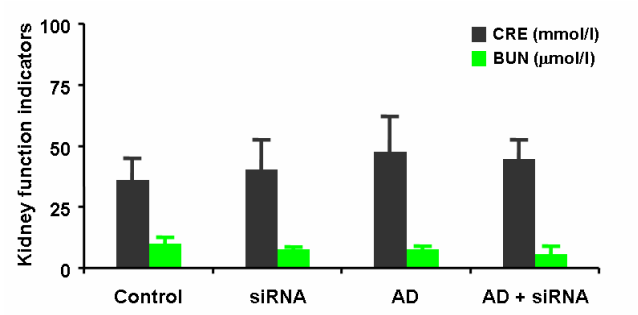
Kidney function indicators
100
75
50
25
0
CRE (mmol/l)
BUN (μmol/l)
Control
siRNA
AD
AD + siRNA

D

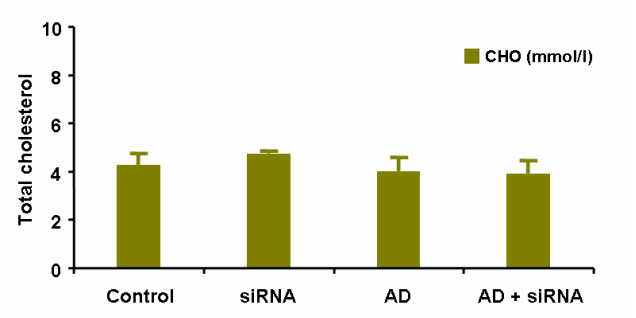
Total cholesterol
10
8
6
4
2
0
CHO (mmol/l)
Control
siRNA
AD
AD + siRNA

Figure S13: Schematic representation of the coarse-grained DPD model of the **AD** dendron. The different bead types are colored as follows: RC, dark magenta; R, plum; L, dark turquoise; G, chartreuse; C, light gray (see SI text for details).

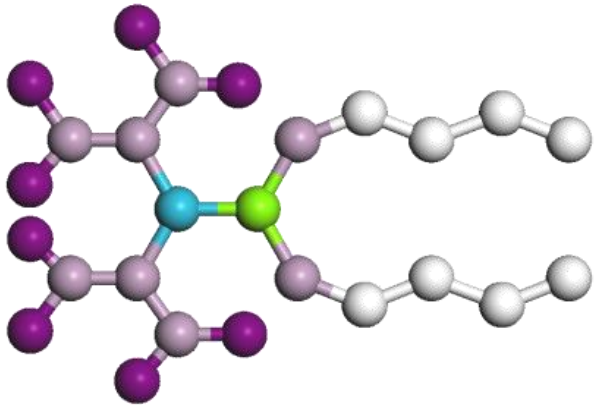

Table S1: DPD interaction parameters used in this work.

	RC	R	L	G	C	S	W
RC	41						
R	31	27					
L	33	34	31				
G	46	42	47	26			
C	80	82	40	60	22		
S	10	35	38	33	74	45	
W	22	31	65	29	82	20	25

Synthesis and characterization of amphiphilic dendrimers: The chemical reagents were purchased from Acros Organics, Sigma Aldrich or Alfa Aesar. The ^{1}H NMR and ^{13}C NMR spectra were recorded at Varian Mercury-VX300 or 600 spectrometers or Bruker Avance I-500MHz spectrometer at room temperature. Coupling constants (*J*) are reported in Hertz, and chemical shifts are reported in parts per million (ppm) with TMS as an internal reference. FAB and ESI mass spectra were determined using ZAB-HF-3F or Finnigan LCQ Advantage mass respectively. MALDI-TOF mass spectra were recorded on a Voyager DE-STR. IR spectra were recorded with a Nicolet 380 spectrophotometer. Methyl acrylate, ethylenediamine, tetrahydrofuran and dimethylformamide (DMF) were distilled before use. All other reagents and solvents were used without any further purification from commercial sources. The compound **2-1** was synthesized according to the reported literature.[1]

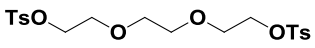

1-1

1-1: To a solution of triethyleneglycol (2.00 g, 13.3 mmol) and triethylamine (4.60 mL, 33.1 mmol) in CH_2Cl_2 (5.00 mL) was added dropwise *p*-toluenesulfonyl chloride (6.13 g, 32.2 mmol) in CH_2Cl_2 (20.0 mL) at 0 ℃. The reaction solution was stirred for 20 h at 0 ℃ and then diethyl ether (20.0 mL) was added into the reaction mixture. The mixture was filtered, concentrated and the residue was purified by column chromatography eluting with Petroleum ether/EtOAc (2:1) to give **1-1** (5.53 g, 91%) as a white solid.

^{1}H NMR (300 MHz, $CDCl_3$): δ 7.79 (d, 4H, *J* = 8.1 Hz, Ar-H), 7.34 (d, 4H, *J* = 8.1 Hz, Ar-H), 4.14 (t, 4H, *J* = 4.4 Hz, CH_2), 3.65 (t, 4H, *J* = 4.4 Hz, CH_2), 3.53 (s, 4H, CH_2), 2.44 (s, 6H, CH_3); ^{13}C NMR (75 MHz, $CDCl_3$): δ 145.1, 133.2, 130.1, 128.2, 70.9, 69.4, 69.0, 21.8.

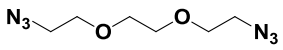

1-2

1-2: To a solution of **1-1** (5.91 g, 12.9 mmol) in acetone (26.6 mL) and H_2O (10.0 mL), NaN_3 (4.20 g，64.6 mmol) was added in a portion and the reaction mixture was stirred at 80 ℃ for 24 h. The reaction mixture was allowed to cool to room temperature, after removal of the acetone, H_2O (15.0 mL) was added. The aqueous phase was extracted with CH_2Cl_2 (15.0 mL×3), and the organic phase was combined, dried over anhydrous $MgSO_4$, and concentrated in vacuo. The resulting crude product was purified by column chromatography eluting with Petroleum ether/EtOAc (2:1) to give **1-2** (2.54 g, 98%) as a colorless oil.

^{1}H NMR (300 MHz, $CDCl_3$): δ 3.69 (m, 8H, CH_2), 3.40 (t, 4H, *J* = 4.4 Hz, CH_2); ^{13}C NMR (75MHz, $CDCl_3$): δ 70.8, 70.2, 50.7; IR (cm^{-1}): υ 2106.4 (-N_3); MS-FAB: *m*/*z* 201 $[M+H]^+$.

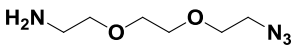

1-3

1-3: To a solution of **1-2** (2.54 g, 12.7 mmol) in ethyl acetate (65.0 mL) and 1N HCl (13.0 mL) was added triphenylphosphine (3.53 g, 13.5 mmol). The reaction solution was stirred at 25 ℃ under argon for 16 h. H_2O (10.0 mL) was added into the reaction mixture, and the aqueous layer was separated and extracted with ethyl acetate (10.0 mL×5). Then the pH of the aqueous phase was adjusted to 13. After removal of the solvent, the resulting residue was dissolved in CH_2Cl_2 (20.0 mL), dried over anhydrous Na_2SO_4, and concentrated under reduced pressure to give **1-3** (1.55 g, 70%) as a colorless oil.

^{1}H NMR (300 MHz, $CDCl_3$): δ 3.63-3.67 (m, 6H, CH_2), 3.50 (t, 2H, *J* = 5.1 Hz, CH_2), 3.37 (t, 2H, *J* = 5.1 Hz, CH_2), 2.85 (t, 2H, *J* = 4.8 Hz, CH_2), 1.98 (s, 2H, NH_2); ^{13}C NMR (150MHz, $CDCl_3$): δ 73.7, 70.9, 70.5, 70.3, 50.8, 42.0; IR (cm^{-1}): υ 2107.6 (-N_3); MS-ESI: *m*/*z* 175.1 $[M+H]^+$.

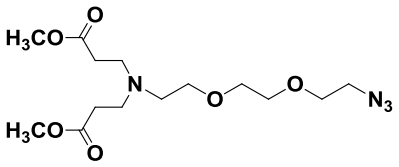

1-4

1-4: To a solution of **1-3** (444 mg, 2.55 mmol) in methanol (5.00 mL) was added methyl acrylate (549 mg, 6.38 mmol) in methanol (2.00 mL) at 0 ℃. The reaction solution was stirred for 2 h at 0 ℃ and for an additional 48 h at 30 ℃ under argon. The reaction solution was evaporated, and then the resulting residue was purified by column chromatography eluting with Petroleum ether/EtOAc (2:1) to give **1-4** (702 mg, 80%) as a colorless oil.

^{1}H NMR (300 MHz, $CDCl_3$): δ 3.62-3.69 (m, 12H, CH_2, CH_3), 3.53 (t, 2H, *J* = 6.3 Hz, CH_2), 3.39 (t, 2H, *J* = 4.7 Hz, CH_2), 2.83 (t, 4H, *J* = 7.4 Hz, CH_2), 2.68 (t, 2H, *J* = 6.2 Hz, CH_2), 2.46 (t, 4H, *J* = 7.4 Hz, CH_2); ^{13}C NMR (150MHz, $CDCl_3$): δ 173.2, 70.9, 70.7, 70.2, 69.9, 53.4, 51.8, 50.9, 50.1, 32.8; IR (cm^{-1}): υ 2104.6 (-N_3); MS-ESI: *m*/*z* 347.1 $[M+H]^+$. HRMS: calcd for $C_{14}H_{27}N_4O_6$ $[M+H]^+$ 347.1925, found 347.1928.

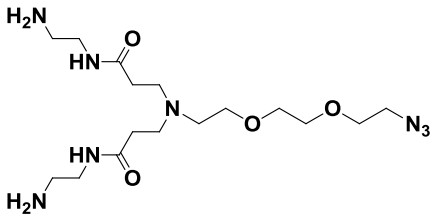

1-5

1-5: To a solution of **1-4** (95.6 mg, 0.276 mmol) in methanol (1.00 mL) was added ethylenediamine (5.00 mL, 74.6 mmol). The reaction solution was stirred for 24 h at 30 ℃ under argon and monitored with IR until the reaction reached completion. After removal the solvent, the resulting residue was purified by precipitation with CH_3OH/Et_2O three times to give **1-5** quantitatively (111 mg) as a colorless oil.

^{1}H NMR (300 MHz, $CDCl_3$): δ 7.42 (br s, 2H, NH), 3.62-3.68 (m, 6H, CH_2), 3.55 (t, 2H, *J* = 5.1 Hz, CH_2), 3.40 (t, 4H, *J* = 4.7 Hz, CH_2), 3.26-3.31 (m, 4H, CH_2), 2.76-2.84 (m, 8H, CH_2), 2.67 (t, 2H, *J* = 5.6 Hz, CH_2), 2.37 (t, 2H, *J* = 6.2 Hz, CH_2),

1.91 (s, 4H, NH_2); ^{13}C NMR (150MHz, $CDCl_3$): δ 173.0, 70.9, 70.5,70.2, 69.5, 53.7, 51.1, 50.9, 42.2, 41.6, 34.5; IR (cm^{-1}): υ 2110.0 ($-N_3$); MS-ESI: *m*/*z* 403.2 $[M+H]^+$; HRMS: calcd for $C_{16}H_{34}N_8O_4Na^+$ $[M+Na]^+$ 425.2595, found 425.2586.

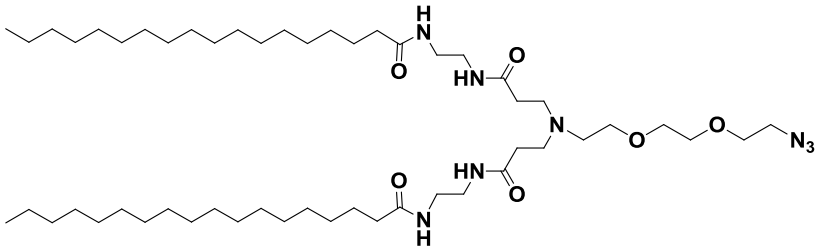

1

1: To a solution of stearic acid (455 mg, 1.60 mmol) in THF (10.0 mL) was added *N,N'*-carbonyldiimidazole (260 mg, 1.60 mmol). The reaction mixture was stirred for 30 min at 60 ℃. Then to this reaction mixture a solution of **1-5** (260 mg, 0.646 mmol) in DMF (4.00 mL) was added, and the reaction was stirred for another 20 h at 60 ℃ under argon. After cooling to room temperature, ethyl acetate (70.0 mL) was added into the reaction mixture, and the obtained solution was kept at -20 ℃ for 3 h. The precipitation was filtered, and dried under reduced pressure to give **1** (476 mg, 79 %) as a white solid.

^1H NMR (300 MHz, $CDCl_3/CD_3OD$ = 5:1): δ 3.64-3.68 (m, 8H, CH_2), 3.54-3.58 (m, 6H, CH_2), 3.37-3.42 (m, 4H, CH_2), 2.77 (t, 4H, *J* = 6.5 Hz, CH_2), 2.69 (t, 2H, *J* = 4.8 Hz, CH_2), 2.34 (t, 4H, *J* = 6.0 Hz, CH_2), 2.17 (t, 4H, *J* = 7.2 Hz, CH_2), 1.59 (br, 4H, CH_2), 1.26 (br, 56H, CH_2), 0.88 (t, 6H, *J* = 6.3 Hz, CH_3); ^{13}C NMR (150 MHz, $CDCl_3/CD_3OD$ = 5:1): δ 175.2, 175.1, 174.0, 70.6, 70.3, 70.0, 68.9, 52.8, 50.7, 50.3, 39.4, 38.9, 36.6, 33.6, 32.0, 29.8, 29.6, 29.4, 25.9, 22.7, 14.1; IR (cm^{-1}): υ 2108.3 ($-N_3$); MS-ESI: *m*/*z* 935.7 $[M+H]^+$; HRMS: calcd for $C_{52}H_{103}N_8O_6^+$ $[M+H]^+$ 935.7995, found 935.7978.

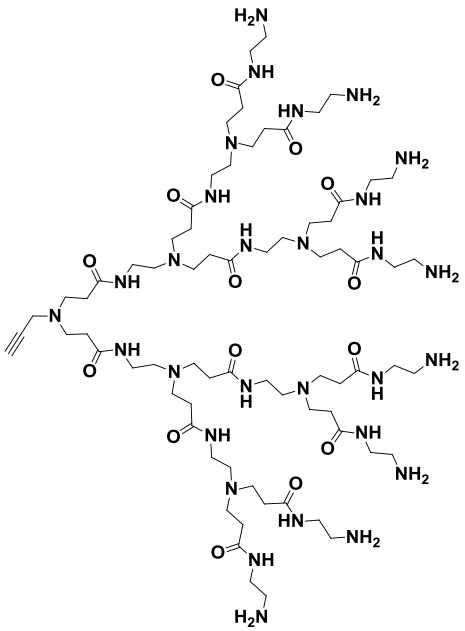

2

2: To a solution of **2-1** (138.7 mg, 0.10 mmol, 1 eq) in methanol (5 mL) was added ethylenediamine (0.26 mL, 3.89 mmol, 39 eq). The reaction mixture was stirred under argon for 72 h at 30 ℃ and monitored by IR until the reaction reached completion. The reaction solution was evaporated, and then the residue was purified by precipitation with CH_3OH/Et_2O three times, yielding **2** (158.5 mg, 98.6%) as yellow viscous oil. ^1H NMR (600 MHz, CD_3OD): 3.45 (s, 2H, CH_2), 3.22-3.24 (m, 28H, CH_2), 2.70-2.80 (m, 44H, CH_2), 2.55-2.58 (m, 12H, CH_2), 2.36-2.34 (m, 28H, CH_2); 2.20 (br, 1H, CH); ^{13}C NMR (75 MHz, CD_3OD): δ 174.1, 173.7, 173.4, 52.3, 49.9, 49.5, 48.7, 45.2, 41.8, 41.1, 40.8, 37.4, 33.6; HRMS: calcd. for $C_{73}H_{148}N_{29}O_{14}^{3+}$ $[M+3H]^{3+}$ 551.7248, found 551.7263.

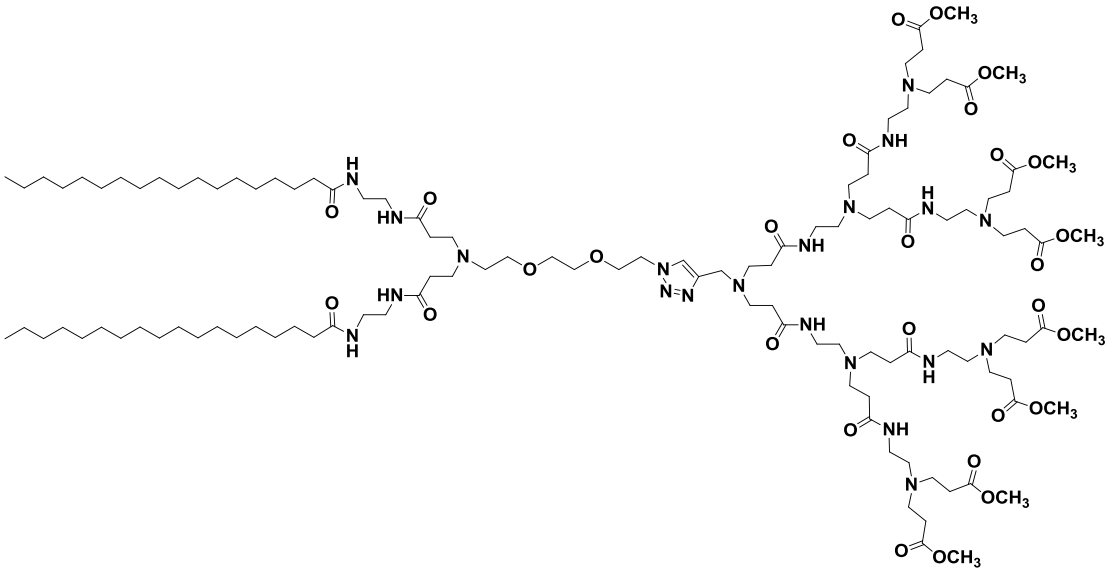

AD-1

AD-1: To a solution of **1** (92.0 mg, 0.0644 mmol) in DMF (5.00 mL) were added **2-1** (58.7 mg, 0.0627 mmol) and CuI (3.60 mg, 0.0190 mmol) successively. The vessel was sealed and purged with argon for 5 min, and then 1.8-diazabicyclo(5,4,0)undec-7-ene (DBU) (70.0 μL, 0.468 mmol) was added into the reaction mixture. The resulting mixture was stirred at 60 ℃ for 3 h until the reaction was completed indicated by IR analysis. DMF was removed under reduced pressure. The obtained residue was suspended in 15.0 mL saturated NH_4Cl solution and extracted with CH_2Cl_2 (15.0 mL×3). The combined organic layers were washed successively with saturated NH_4Cl solution (15.0 mL×2), saturated $NaHCO_3$ solution (15.0 mL×2) and brine (20.0 mL). The organic phase was dried with $MgSO_4$ and concentrated. The crude product was purified by precipitation with CH_2Cl_2/Et_2O at -20 ℃ for 16 h. The precipitate was the collected, washed with Et_2O and dried under vacuum, giving **AD-1** (108 mg, 73%) as a white solid.

^{1}H NMR (600 MHz, $CDCl_3$): δ 7.89 (br s, 2H, NH), 7.78 (br s, 2H, NH), 7.73 (s, 1H, CH), 7.08 (br s, 4H, NH), 7.01 (br s, 2H, NH), 4.53 (t, 2H, *J* = 4.8 Hz, CH_2), 3.87 (t, 2H, *J* = 4.8 Hz, CH_2), 3.82 (s, 2H, CH_2), 3.66 (s, 24H, CH_3), 3.53-3.56 (br, 4H, CH_2), 3.46 (t, 2H, *J* = 4.5 Hz, CH_2), 3.34 (br , 8H, CH_2), 3.26-3.29 (m, 12H, CH_2), 2.73-2.81 (m, 32H, CH_2), 2.52-2.62 (m, 14H, CH_2), 2.33-2.44 (m, 32H, CH_2), 2.16 (t, 4H, *J* = 7.8 Hz, CH_2), 1.58 (br, 4H, CH_2), 1.25 (br, 56H, CH_2), 0.87 (t, 6H, *J* = 7.2 Hz, CH_3);

^{13}C NMR (150 MHz, $CDCl_3$): δ 174.4, 173.7, 173.3, 172.6, 143.9, 124.2, 70.7, 70.4, 69.6, 69.1, 53.1, 52.6, 51.9, 50.8, 50.3, 50.0, 49.4, 47.8, 40.3, 39.3, 37.6, 37.4, 36.9, 34.2, 34.0, 33.8, 32.9, 32.1, 29.9, 29.8, 29.7, 29.6, 26.0, 22.9, 14.4; IR (cm^{-1}): υ 1734.4 (-C=O, ester), 1642.9(-C=O, amide); HRMS: calcd for $C_{117}H_{216}N_{21}O_{28}^{+}$ $[M+H]^{2+}$ 2363.1082, found 2364.2357.

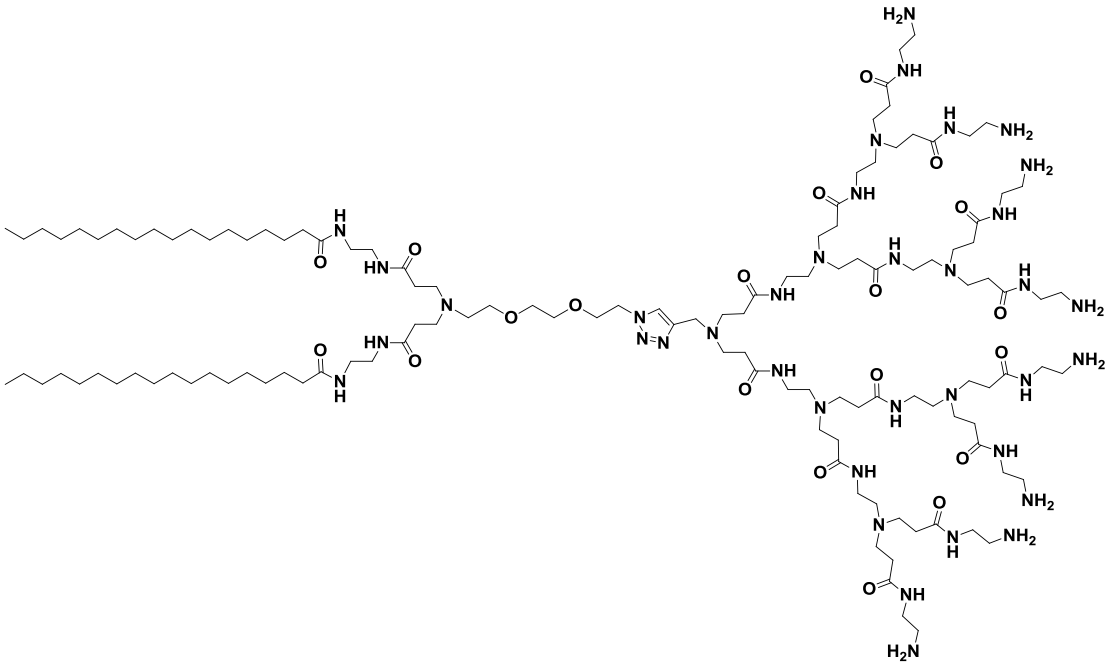

AD

AD: To a solution of **AD-1** (63.2 mg, 0.0267 mmol) in methanol and CH_2Cl_2 (6.00 mL, v:v=1:1) was added ethylenediamine (2.00 mL, 29.9 mmol). The reaction mixture was stirred for 72 h at 30 ℃ under argon. When the reaction was completed indicated by IR analysis, the reaction solution was evaporated, the obtained residue was dissolved in a small amount of mixed solvent of methanol and DCM (v:v=1:1) and then precipitated in Et_2O for three times. The crude product was further purified by dialysis using dialysis tube of MWCO 2000, followed by lyophilization to give **AD** (55.9 mg, 81%) as a white solid.

^{1}H NMR (600 MHz, $CD_3OD/CDCl_3$ = 3:2): δ 7.95 (s, 1H, CH), 4.56 (br, 2H, CH_2), 3.88 (br, 2H, CH_2), 3.82 (s, 2H, CH_2), 3.56-3.58 (m, 6H, CH_2), 3.46-3.48 (m, 16H, CH_2), 3.24-3.29 (m, 20H, CH_2), 3.06-3.08 (m, 16H, CH_2), 2.75-2.88 (m, 34H, CH_2), 2.61 (br, 12H, CH_2), 2.40-2.44 (m, 32H, CH_2), 2.15 (t, 4H, *J* = 7.2 Hz, CH_2), 1.56 (br,

4H, CH_2), 1.23 (br, 56H, CH_2), 0.85 (t, 6H, *J* = 6.6 Hz, CH_3); ^{13}C NMR (125 MHz, $CD_3OD/CDCl_3$ =3:2): δ 174.7, 173.7, 173.4, 172.7, 149.1, 124.1, 69.9, 69.7, 68.8, 68.4, 51.8, 49.6, 49.5, 39.6, 38.6, 38.4, 36.9, 35.9, 33.2, 32.3, 31.4, 29.2, 29.1, 29.0, 26.9, 26.8, 25.4, 22.1, 13.4. IR (cm^{-1}): υ 1644.4 (-C=O), 1556.1 ($-NH_2$); HRMS: calcd. for $C_{125}H_{248}N_{37}O_{20}^{+}$ $[M+H]^+$ 2587.9521, found 2588.1735.

Experimental section

Materials. The sequence of Hsp27 siRNA (Thermo Fisher Scientific, Illkrich, France) used corresponded to the human Hsp27 site (Sense: 5'-GCU GCA AAA UCC GAU GAG AC dTdT-3'; antisense: 5'-GUC UCA UCG GAU UUU GCA GC dTdT-3'). A scrambled siRNA duplex (Sense: 5'-CUU ACG CUG AGU ACU UCG A dTdT-3', antisense: 5'-UCG AAG UAC UCA GCG UAA G dTdT-3') (Thermo Fisher Scientific) was used as a control for in vitro. The siGENOME negative control D-001210-01 (Thermo Fisher Scientific) was used as a scramble control for in vivo. The Dy-647 labeled Hsp27 siRNA was purchased from Thermo Fisher Scientific. The allStars non-silencing siRNA modified with 3' Alexa 488 via aminohexyl-linker was obtained from Qiagen (Courtaboeuf, France). The Dicer substrate siRNAs (dsiRNAs) including Anti-CD4 dsiRNA (Sense: 5'-GAU CAA GAG ACU CCU CAG UGA GAA G-3'; antisense: 5'-CUU CUC ACU GAG GAG UCU CUU GAU CUG-3' (2'-OMe modified U was underlined)), Anti-*tat/rev* dsiRNA (Sense: 5'-GCG GAG ACA GCG ACG AAG AGC UCA UCA-3'; antisense: 5'-UGA UGA GCU CUU CGU CGC UGU CUC CGC dTdT-3'), mutant dsiRNA (Sense: 5'-GCG CUA ACA GCG UGU AAG AGC GAC UCA -3'; Antisense: 5'- UGA GUC GCU CUU ACA CGC UGU UAG CGC UU -3' (The mutated sequences were underlined)), Anti-STAT3 dsiRNA (Sense: 5'- GGA AGC UGC AGA AAG AUA CGA CUga -3'; Antisense: 5'- UCA GUC GUA UCU UUC UGC AGC UUC CGU -3') and irrelative dsiRNA (NC1 dsiRNA) were purchased from Integrated DNA Technologies (Coralville, IA, USA). The siRNA (Sense: 5'- CCU UGA GGC AUA CUU CAA AdTdT -3'; Antisense: 5'- UUU GAA GUA UGC CUC AAG GdTdT -3') used for in vivo toxicity evaluation was obtained from Suzhou Ruibo (Suzhou, China).

Ethidium bromide, RNase, endocytosis inhibitors (cytochalasin D, genistein and chlorpromazine), paraformaldehyde, bovine serum albumin (BSA) dioleoylphosphatidylethanolamine (DOPE), chloroquine, bafilomycin A1 and 3-(4,5-dimethylthiazol-2-yl)-2,5-diphenyltetrazolium bromide (MTT) were supplied by Sigma-Aldrich (Saint-Quentin Fallacier, France). MTS test kit (CellTiter 96®

Non-Radioactive Cell Proliferation) was obtained from Promega (Madison, WI, USA). Lipofectamine RNAiMAX (lipo), oligofectamine (oligo), endocytic markers (Alexa-Fluor® 647-labeled dextran, transferrin, and cholera toxin B), Alexa-Fluor® 647-labeled Phalloidin, 4', 6'-diamidino-2-phenylindole (DAPI) and Hoechst 34580 were purchased from Invitrogen (Invitrogen Ltd, Paisley, UK). Tran IT-TKO (TKO) was obtained from Mirus Bio LLC (Madison, WI, USA). PE Annexin V and 7-aminoactinomycin D (7-AAD) were purchased from BD Pharmingen (Le pont de claix, France). All other reagents and solvents of analytical grade were used without further purification from commercial sources.

Cell culture: Human prostate cancer PC-3 cells were purchased from the American Type Culture Collection (ATCC) (Manassas, VA, USA). PC-3 cells were maintained in DMEM (Lonza Group Ltd., Switzerland), supplemented with 10% fetal bovine serum (FBS) (Lonza). Breast cancer cell lines MDA-MB431 and MCF-7 were gifts from Dr. Daniel Birnbaum and Mr. Julien Wicinski (Institut Paoli-Calmettes, Marseille, France). MDA-MB431 cells were maintained in RPMI 1640 (Invitrogen), supplemented with 10% FBS, MEM non-essential amino acids (NEAA) (Life technologie SAS), HEPES (Life technologie SAS), ANTI-ANTI (Life technologie SAS). MCF-7 cells were maintained in RPMI 1640 (Invitrogen), supplemented with 10% FBS, MEM non-essential amino acids (NEAA) (Life technologie SAS), HEPES (Life technologie SAS), ANTI-ANTI (Life technologie SAS), insulin humalog (50 μg/mL). CCRF-CEM cells were purchased from ATCC and cultured in RPMI 1640 supplemented with 10% FBS. Human mantle cell lymphoma (MCL) (Jeko-1 cells) was purchased from ATCC and cultured in RPMI 1640 supplemented with 20% FBS. Cells were cultured in a humidified 5% CO_2 incubator at 37 ℃. Peripheral blood mononuclear samples were obtained from healthy donors from the City of hope National Medical Center. PBMCs were isolated from whole blood by centrifugation through a Ficoll-Hypaque solution (Histopaque-1077, Sigma). CD4 cells (T-cytotoxic/suppressor cells) were depleted from the PBMCs by CD4 Dynabeads (Invitrogen, CA, USA) according to the manufacturer's instructions. CD4+ T

cell-depleted PBMCs were washed twice in PBS and resuspended in culture media (RPMI 1640 with 10% FBS, 1×PenStrep and 100 U/mL interleukin-2). CD34+ hematopoietic stem cells are enriched from umbilical cord blood or bone marrow by anti-CD34 antibody-coupled magnetic beads (Miltenyi Biotech, Aubum, CA, USA). CD34+ cells are cultured in Iscove's modified Dulbecco's medium (IMDM) supplemented with 20% BIT9500 (Stem Cell Technology, Vancouver, BC, Canada), 40 mg/mL human low density lipoproteins, 10^{-4} M 2-mercaptoethanol, 100 ng/mL SCF, 100 ng/mL flt3-ligand, 10 ng/mL TPO (PeproTech, Rocky Hill, NJ), 20 ng/mL IL-3, 20 ng/mL IL-6. Cells should be cultured on the Non-Tissue Culture Treated plates (Becton Dickinson Labware) for 7-10 days before assay. Human glioma stem cells (GSCs) (PBT003) were cultured in DMEM-F12 medium (Omega Scientific) supplemented with 1X B27 (Invitrogen), 5 μg/ml heparin (Sigma), 2 mM L-glutamine (Media Tech), 27.4 mM HEPEs (Fisher), 20 ng/ml EGF (PeproTech) and 20 ng/ml FGF (PeproTech). Cells were maintained at 37 ℃ in a 5%CO_2 humidified atmosphere.

Critical micelle concentration (CMC): CMC was determined using pyrene as a fluorescence probe. Dendrimer solutions at different concentrations varied from 1.26×10^{-7} to 1.00×10^{-3} mol/L were prepared and the final pyrene concentration was 6×10^{-7} mol/L in water. The solutions were sonicated for 30 min and kept for 2 h at room temperature to promote the micelle formation prior to fluorescence measurement. Fluorescence spectra were recorded at the emission wavelength of 334 nm on F-4500 fluorescence spectrophotometer at room temperature. Excitation and emission bandwidths were 5 nm. The fluorescence intensity ratio of I_{373}/I_{383} was analyzed as a function of micelle concentration.

Potentiometric pH titration: The solution of amphiphilic dendrimer **AD** (2 mmol in 10 mL) was adjusted to pH around 2-3 with 0.5 M HCl, pH titration was carried out with 0.1 M NaOH using Mettler Toledo 320-S pH meter.

Dynamic light scattering (DLS): The siRNA solution was mixed with indicated amount of amphiphilic dendrimer solution at N/P ratio 10. The final concentration of

the siRNA was 1 μM. After incubated at 37 ℃ for 30 min, size distribution and zeta potential measurement was performed using Zetasizer Nano-ZS (Malvern, Ltd. Malvern, U. K.) with a He-Ne ion laser of 633 nm.

Transmision electronic microscopy (TEM): 10 μL of a solution of siRNA (5 ng/μL) were mixed with 10 μL of a solution of dendrimer **AD** in MiliQ water at N/P ratio of 10. After equilibration (30 min), 4 μL of this mixture were dropped on a standard carbon-coated copper TEM grid, and then allowed to dry in air (15-20 min, under light heating). The grid was stained with 3 μL uranyl acetate (2% in 50%EtOH) for 5 sec, and the excess uranyl acetate was removed by filter paper. The dried specimens were observed with a JEOL 3010 transmission electron microscope operating at 300 kV. Data were analyzed with Digital Micrograph software.

Langmuir isotherm: The Langmuir isotherm was obtained using a home-made teflon trough. The teflon trough was thoroughly cleaned till it was rendered perfectly hydrophobic. It was then filled with 12 mM phosphate buffer at pH=7.4 prepared using ultrapure water (Elga, UK). The dendrimer was dissolved in chloroform to a concentration of 125 μg/mL. The dendrimer solution was carefully added dropwise onto the surface of the buffer (the air/water interface). The pressure was recorded using a Wilhelmy plate until it reached a stable state. The experiment was repeated three times.

Electro-swelling method to prepare giant vesicles: A home-made teflon chamber was used to form giant vesicles by electro-swelling. 100 μL the lipid solution dissolved in chloroform was coated on previously cleaned ITO-coated glass plates. The solvent was evaporated overnight under vacuum. Then the plates were placed in the chamber (separated by teflon spaces of 1 mm thickness) and the chamber was filled with sucrose solution (300 mM). An AC voltage of 1.7 V peak-to-peak and at frequency of 10 Hz was applied for 2 h. The vesicles were harvested and observed in a chamber with glucose solution using phase contrast microscopy (63 X antiflex objective on a Axiovert microscope, Carl Zeiss, Germany). The images were recorded with a CCD camera (Andor, Ireland) and presented without further treatment.

Ethidium bromide exclusion assay: In a 96 well plate, 1.00 μg ethidium bromide and 1.32 μg siRNA were mixed in PBS buffer to achieve a total volume of 50 μL at pH 7.4. The plate was incubated at 25 ℃ for 15 min, then appropriate amount of dendrimer solution together with PBS buffer solution were added to achieve a total volume of 100 μL with the final concentration of ethidium bromide at 25.4 μM, siRNA at 20.0 μM per base pair and the desired dendrimer concentrations. This plate was further incubated at 25 ℃ for 30 min before exciting at 560 nm. The fluorescence emission was recorded at 590 nm (Fluostar OPTMA, BMG LABTECH, Germany). The fluorescence values were normalized to wells containing only siRNA and ethidium bromide. Experiments were performed in triplicate.

Gel retardation analysis: The dendrimer was diluted to an appropriate concentration and stored at 4 ℃. The siRNA was diluted with H_2O. Both solutions were mixed at various N/P ratios (= [total terminal amines in the dendrimer **AD**]/[phosphates in the siRNA]) from 1:5 to 10:1 and incubated at 37 ℃ for 30 min. The final concentration of siRNA was adjusted to 200 ng/well. siRNA/amphiphilic dendrimer complexes were analyzed by electrophoretic mobility-shift assays in 1.2% agarose gel in standard TBE buffer. The siRNA bands were stained by ethidium bromide and then detected by a Herolab EASY CCD camera (type 429K) (Herolab, Wiesloch, Germany).

Stability of siRNA/amphiphilic dendrimer complex against RNase A: An aliquot of 2.4 μg of siRNA and the indicated amounts of amphiphilic dendrimer **AD** at N/P ratio 10 was kept at 37 ℃ for 30 min. Then the complexes were incubated in the presence of 0.01 μg/mL RNase A at 37 ℃ for 0, 5, 10, 15, 20, 30, 45, 60, 75, 90, 105 and 120 min. Aliquots (4 μL) of the corresponding solution were withdrawn, added to 1.5 μL of 1% SDS solution on the ice and then subjected to electrophoresis in 1.2% agarose gel in standard TBE buffer. The siRNA bands were stained by ethidium bromide and then detected by a Herolab EASY CCD camera (type 429K) (Herolab, Wiesloch, Germany).

Uptake of siRNA/AD complexes in PC-3 cells

Confocal microscopy.

The living cell confocal microscopy was used to evaluate cellular uptake and intracellular location of complexes. PC-3 cells were seeded at a density of 10×10^4 cells/chamber in 4-well glass chamber slides (Lab-Tek, Thermo Fischer Scientific, Illkirch, France) one day before using. Preparation of the siRNA/amphiphilic dendrimer **AD** complexes was performed as indicated above. Then, the complex containing Alexa488 labeled non-silencing siRNA was added to the cells in Opti-MEM transfection medium. After 4 h incubation at 37 ℃, cells were washed with PBS and stained with Hoechst 34580. For cell uptake in presence of endocytosis markers, the Alexa-Fluor® 647-labeled markers were added during the final 15 minutes incubation of siRNA/dendrimer **AD** nanaoparticles prior to nuclear staining with Hoechst 34580. For observation of actin rearrangement, after incubation for 15 min at 37 ℃ with siRNA/dendrimer **AD** nanaoparticles, cells were fixed in 4% paraformaldehyde, permeabilized with 0.1% triton, incubated with 1% bovine serum albumin (BSA) and stained with Alexa-Fluor® 647 phalloidin to label actin fibers, then with DAPI to label the nuclei. A Zeiss LSM 510 Meta laser scanning confocal microscope equipped with inverted Zeiss Axiovert 200 M stand (Carl Zeiss GmbH, Jena, Germany) was used for visualization. Images were acquired using LSM 510 software (Carl Zeiss GmbH).

Flow cytometry.

The uptake mechanism of the siRNA/dendrimer **AD** nanoparticles was examined by means of specific inhibitors of different endocytic pathways. For inhibition experiments, the cells were seeded at a density of 3×10^5 cells in 3.5-cm dishes (Nunc, USA) one day before, then they were incubated with one of following inhibitors: cytochalasin D (to inhibit macropinocytosis), genistein (to inhibit caveolae-mediated endocytosis), or chlorpromazine (to inhibit clathrin-mediated endocytosis) for 1 h in completed medium before the siRNA/dendrimer **AD** complexes were added. Inhibitors were used at concentrations in which they were not cytotoxic for PC-3 cells. After incubation for 15 min at 37 ℃ with 20 nM Alexa488 labeled siRNA/dendrimer **AD** complex (N/P ratio 10), the cell uptake efficiency was measured by flow

cytometry using FACS Calibur (Becton Dickinson (BD), Le Pont de Claix, France). Each assay was performed in triplicate.

In vitro transfection on prostate cancer PC-3 cells and breast cancer MDA-MB231 and MCF-7 cells: One day before transfection, 1.5×10^5 cells were seeded in 6 cm dishes in 4 mL of fresh complete medium containing 10% FBS. Before transfection, a solution of the Hsp27 siRNA/amphiphilic dendrimer complex was prepared accordingly. The desired amount of Hsp27 siRNA and amphiphilic dendrimer was diluted in 200 µL of Opti-MEM tranfection medium. The solutions were mixed with a vortex for 10 s, and then left for 10 min at room temperature. The amphiphilic dendrimer was added to the siRNA solution, homogenized for 10 s with a vortex and left 30 min at room temperature. Then 1.6 mL serum-free medium was added into the complex solution and the final volume brought to 2 mL. Before addition of the transfection complexes, the complete medium with serum was removed and cells were washed with PBS once. Then, 2 mL of the complex solution was added and incubated at 37 ℃ in the absence of 10% FBS. After 8 h of incubation, the transfection mixture was replaced with the complete medium containing 10% FBS, and maintained under normal growth conditions for further incubation of 48 h for qRT-PCR assay or 72 h for western blot assay. Transfection of siRNA using commercial transfection reagent oligofectamine was performed by following the manufacturers' instruction. Western blot assay was carried out 72 h post-transfection.

Effect of dioleoylphosphatidylethanolamine (DOPE)

The transfection experiments involving DOPE were performed as described above, except the desired amount of the amphiphilic dendrimer was pre-mixed with DOPE at different ratios (mole/mole) and equilibrated at room temperature for 10 min before diluting in 200 µL of Opti-MEM tranfection medium for the complexation with Hsp27 siRNA

Effect of bafilomycin A1

The transfection experiments involving bafilomycin A1 were performed as described above, except that PC-3 cells were pre-incubated with 200 nM bafilomycin A1 for 1 h

at 37 ℃.

Serrum effect

The serum effect was overcome by increasing the N/P ratios and using 50 μM chloroquine. The transfection experiments involving chloroquine were performed as described above, except that PC-3 cells were incubated in the serum-containing medium with the transfection complexes in presence of 50 μM chloroquine at 37 ℃ for 8 h.

Determination of Hsp27 mRNA expression by quantitative real-time (qRT)-PCR:

The expression of the Hsp27 mRNAs was analyzed by quantitative real-time PCR amplification analysis as previously described.[2] Briefly, total RNAs were isolated using the Trizol method (Invitrogen, Ltd., Paisley, U.K.). Then 1 μg of RNAs was reverse-transcribed into cDNA by using ImProm-α Reverse Transcription system (Promega) (0.5 μg of oligo dT primer, 1 μL ImProm-α reverse transcriptase, 0.5 μL of RNase inhibitor, 1 μL of 10 mM dNTP mix, 4.8 μL of 25 mM $MgCl_2$, 4 μL of 5× RT buffer) in a final volume of 20 μL. The thermal cycling protocol employed included two steps (step 1, 70 ℃ for 5 min, and 4 ℃ for 5 min; step 2, 25 ℃ for 5 min, 42 ℃ for 1 h, 70 ℃ for 15 min, and 4 ℃ forever).

The real-time PCR was conducted using the LightCycler 2.0 instrument (Roche Diagnostics, GmbH Mannheim, Germany). Reaction mixtures contained total volume of 20 μL consisting of 5 μL of each diluted cDNA (1:10), 10 μL of SYBR Premix Ex Taq (2×) (TaKaRa Bio. Inc., Japan), 0.4 μL of primers F and primers R (10 μM) of target gene and internal control 18S, and 4.2 μL of H_2O. The sequences of primers are as follows: Hsp27 primer F: 5'-TCCCTGGATGTCAACCACTTC-3' and primer R: 5'-TCTCCACCACGCCATCCT-3'; 18S primer F: 5'-CTACCACATCCAAGGAAGGC-3' and primer R: 5'-TTTTCGTCACTACCTCCCCG-3' (Eurogentec, S. A., Seraing, Belgium). The conditions were as follows: an initial denaturation step at 95 ℃ for 10 s; then 45 cycles of 95 ℃ for 5 s, 57 ℃ for 6 s, and 72 ℃ for 12 s. A melting curve was carried out after an amplification programme by heating at temperatures from 65 to 95 ℃ in

1.5 min. A final cooling step at 40 ℃ for 1 min was performed. Each sample was analyzed in triplicate in the PCR reaction to estimate the reproducibility of data. The data was acquired by using Roche Molecular Biochemicals light cycler software version 3.5 and statistical analysis was obtained by RelQuant (Roche).

Determination of Hsp27 protein expression by western blot analysis: Samples containing equal amounts of protein (15 μg) from lysates of cultured PC-3 cells or tumors were analyzed by Western blot analysis as described previously with 1:5000-diluted anti-human Hsp27 rabbit polyclonal antibody (Enze Life Sciences, Villeurbanne, France), 1:1000-diluted anti-human β-Actin rabbit monoclonal antibody (Ozyme, Saint Quentin Yvelines, France), or 1:2000-diluted anti-human vinculin mouse monoclonal antibody (Sigma-Aldrich). Filters were then incubated for 1 h at room temperature with 1:5000-diluted horseradish peroxidase-conjugate anti-rabbit or mouse monoclonal antibody (Santa Cruz Biotechnology Inc., Nanterre, France). Specific proteins were detected using an enhanced-chemiluminescence Western blotting analysis system (GE Healthcare Life Sciences, Velizy-Villacoublay, France).

MTT (3-(4,5-dimethylthiazol-2-yl)-2,5-diphenyltetrazolium bromide) assay: The growth inhibitory effects of Hsp27 siRNA plus amphiphilic dendrimer on PC-3 cells were assessed using the MTT assay (Sigma-Aldrich). Briefly, cells were seeded in 12-well microtiter plates and allowed to attach overnight. Cells were then treated with Hsp27 siRNA/amphiphilic dendrimer **AD** for 8 h. Every 1, 3, and 24 h (for the metabolite toxicity evaluation) and every 24 h over a period of 6 days (for cell proliferation measurement), MTT solution (5 mg/mL in PBS) was added to each well and incubated for another 2-4 h. And then the suspension liquid was removed and cells were resuspended in DMSO. The optical density (OD) of these DMSO solutions was read at 540 nm. The difference of OD values between treated and non-treated cells reflects the viability of cells after treatments and thus stands for the metabolite toxicity. Each assay was performed in triplicate.

The metabolite toxcity of siRNAs plus dendrimers on CEM, PBMC CD4+, CD34+ and PBT003 cells was determined by MTS assay as well. CellTiter 96®

Non-Radioactive Cell Proliferation (Promega) assays were performed according to manufacturer's protocol. Cells were seeded in each well of 96-well microtiter plates and then treated with dendrimer-siRNA complexes. After 48 h of post-transfection with dendrimer-siRNA, 20 μL MTS solution (5 mg/mL in PBS) was added to each well and then incubated with cells for 2 h in the 37 ℃. The absorbance was measured with a Wallack plate reader using the Kamings protocol at 490 nm. The viability was expressed as the ratio of absorbance obtained from transfected cells to non-transfected cells (n=6).

Crystal violet assay: The growth inhibitory effects of Hsp27 siRNA plus amphiphilic dendrimer on PC-3 cells were assessed using the crystal violet assay. Briefly, cells were seeded in 12-well microtiter plates and allowed to attach overnight. Cells were then treated with Hsp27 siRNA/amphiphilic dendrimer **AD** and controls for 8 h. Every 24 h over a period of 6 days, the cells were fixed with 10% glutaraldehyde solution for 10 min at room temperature, then washed gently twice with distilled water. And then the 0.5% crystal violet solution was added into each well and incubated 5 min at room temperature. Then washed off the excess crystal violet by adding in a large volume of water with a transfer pipette, swirling and removing until the water stayed relatively clear (3-6 times). The plate was drained upside down on paper towels, then Sorensen solution was added to solubilize the stain and plate was agitated on orbital shaker for 5 min until color is uniform with no areas of dense coloration in bottom of wells. The OD of these solutions was read at 540 nm. The difference of OD values between treated and non-treated cells reflects the viability of cells after treatments and thus stands for the metabolite toxicity. Each assay was performed in triplicate.

Lactate dehydrogenase (LDH) assay: PC-3 cells were seeded by 5000 cells per well in 96-well plates and cultured overnight. Cells were then treated with Hsp27 siRNA/amphiphilic dendrimer **AD** in the absence of 10% FBS. After 1, 2, 4, 8, 12 and 24 h, the LDH concentration was measured using commercial LDH kit (Cytotoxicity Detection Kit, Roche). The LDH reaction mixture was freshly prepared according to

the manufacturer's protocol (Roche Diagnostics), 100 μL added to each well of a 96-well plate containing 100 μL of blank, control, or cells in culture, and the plate incubated for 30 min at 25 ℃. Control was performed with lysis buffer and medium, and set as 100% and 0% LDH release, respectively. The relative LDH release is defined by the ratio of LDH released over total LDH in the intact cells. All samples were run in triplicate.

Apoptosis assessment by FACS analysis: The PC-3 cells were plated into 6 cm dishes, and treated with Hsp27 siRNA/amphiphilic dendrimer **AD** or scrambled siRNA/amphiphilic dendrimer **AD** using no treatment and amphiphilic dendrimer (**AD**) alone as controls. Following treatment, cells were trypsinized 4 days after, washed twice with cold PBS buffer, resuspended in 100 μL binding buffer (1X) and transferred to a 0.5 mL culture tube.

In each tube, 5 μL of annexinV-PE and 0.5 μL of 7-AAD (7-aminoactinomycin D) were added. Cells were gently vortexed and incubated for 15 min at room temperature (25 °C) in the dark. Next, 100 μL of binding buffer (1×) (10 mM HEPES, 140 mM NaCl, 2.5 mM $CaCl_2$, pH 7.4) was added to each tube and cell suspension was analyzed by flow cytometry. Data was acquired by flow cytometry using FACS Calibur (Becton Dickinson (BD), Le Pont de Claix, France) with CellQuest software and analyzed by FlowJo software (Tree Star, Inc.). Ten thousand cells were analyzed for each sample. Each assay was performed in triplicate.

Caspase-3 activity assay: Caspase-3 activity was analyzed using Caspase-Glo 3/7 assay luminescent kit (Promega) or the Apo-ONE homogeneous caspase-3/7 assay fluorometric kit (Promega). PC-3 cells were seeded in 96-well microtiter plates and allowed to attach overnight. Cells were then treated once daily with Hsp27 siRNA/amphiphilic dendrimer **AD** for 8 h in the absence of 10% FBS. Every 24 h over a period of 3 days, caspase-3 activity was measured by the cleavage of the luminogenic substrate containing the DEVD sequence or the fluorometric substrate Z-DEVD-R110 according to the instructions of the manufacturer (Promega). Next 100 μL of Caspase-Glo 3/7 reagent was added to each well containing 100 μL of blank

control, or cells in culture. The plate was covered with a plate sealer and incubated at room temperature for 1 h before the luminescence of each well was measured. Each experiment was performed in triplicate.

In vitro transfection on CEM, Jeko-1, PBMC, CD34+ and PBT003 cells: 2×10^5 CEM cells, Jeko-1 cells, PBMC CD4+ cells, CD34+ cells or PBT003 cells per well were seeded in 24-well tissue culture plates in 300 μL fresh complete medium containing 10% FBS (PBT003 cells were cultured in the absence of FBS). Before transfection, complexes of dsiRNA/dendrimer reagents were prepared. The desired amount of dsiRNA and dendrimer reagent was diluted in 50 μL of serum-free medium (Opti-MED), respectively. The dendrimer solution was mixed gently and incubated for 10 min at room temperature. After the 10-minute incubation, the diluted dsiRNA and the dendrimer reagent was mixed gently and incubated for 30 minutes at room temperature. The 100 μL of dsiRNA/dendrimer complex was added to each well containing cells and medium and mixed gently by rocking the plate back and forth. The cells were incubated at 37 ℃ in a CO_2 incubator for 24-72 h for the further assay. Transfection of dsiRNA using commercial transfection reagent Tran IT-TKO (TKO) or Lipofectamine RNAiMAX (lipo) was performed by following the manufacturers' instruction. Further assay was carried out 24-72 h post-transfection.

Determination of down-regulation of CD4 levels by flow cytometry: Down-regulation of CD4 levels by dendrimer **AD**/CD4 dsiRNA nanoparticles in CEM cells detected by flow cytometry. Cells were transfected with 50 nM of Anti-CD4 dsiRNA using dendrimers as described above. 48 h post-transfection, the cells were harvested, washed once with PBS and resuspended in 100 μL of ice cold PBS, 0.5% BSA, 0.2% sodium azide. Primary labelled antibody: 0.1-10 μg/mL (10 μL of CD4 antibody [EDU-2] (FITC) (Abcam) is sufficient for labeling of 1×10^6 cells). After incubation at least for 30 min at RT, reaction solutions were centrifuged to remove the supernatants and washed twice with 320 μL of cold PBS, 0.5% BSA, 0.2% sodium azide at RT, and finally resuspended in 350 μL of cold PBS, 0.5% BSA, 0.2% sodium azide at 25 ℃ and spun down at 1500 rpm for 4 min at 25 ℃. Cells were immediately

assayed using flow cytometry keeping the cells in the dark on ice.

Determination of CD4 gene silencing by qRT-PCR assay: For CD4 expression, cells were transfected with 50 nM of Anti-CD4 dsiRNA using dendrimer as described above. 48 h post-transfection, the total RNAs were isolated with STAT-60 (TEL-TEST "B", Friendswood, TX). Expression of the target genes was analyzed by quantitative Real time-PCR using 2× iQ SyberGreen Mastermix (BIO-RAD) and specific primer sets at a final concentration of 400 nM. Primers were as follows: CD4 forward primer: 5' – GCT GGA ATC CAA CAT CAA GG -3'; CD4 reverse primer: 5'- CTT CTG AAA CCG GTG AGG AC -3'; GAPDH forward primer: 5'- CAT TGA CCT CAA CTA CAT G-3'; GAPDH reverse primer: 5'- TCT CCA TGG TGG TGA AGA C-3'. RNA-Stat60 was used to extract total RNA according to the manufacturer's instruction (Tel-Test). Residual DNA was digested using the DNA-free kit per the manufacturer's instructions (Ambion). cDNA was produced using 2 μg of total RNA, Moloney murine leukemia virus reverse transcriptase and random primers in a 15 μL reaction according to the manufacturer's instructions (Invitrogen). GAPDH expression was used for normalization of the qPCR data.

HIV-1 challenges and p24 antigen assay: The CEM cells or PBMCs were infected with HIV NL4-3 (MOI: 0.001) or HIV-1 JR-FL (MOI: 0.005) for 5 days. Prior to transfection, the infected cells were gently washed with PBS three times to remove free virus. 1.0×10^5 infected cells and 1.0×10^5 uninfected cells were mixed and transfected with 50 nM anti-CD4 or anti-*tat/rev* dsiRNA using dendrimers in 24-well plates as previously described. The culture supernatants were collected at the 3rd day. The p24 antigen analyses were performed using a Coulter HIV-1 p24 Antigen Assay (Beckman Coulter) according to the manufacturer's instructions.

Determination of *tat/rev* mRNA silencing (qRT-PCR analysis): For detection of the *tat/rev* mRNA levels, cells were infected with HIV-1 virus as described above. 72 h post-transfection, total RNAs were isolated and expression of the *tat/rev* coding RNAs was analyzed by qRT-PCR as previously described. Primers were as follows: *tat/rev* forward primer: 5'- GGC GTT ACT CGA CAG AGG AG -3'; *tat/rev* reverse primer:

5’- TGC TTT GAT AGA GAA GCT TGA TG -3’; GAPDH expression was used for normalization of the qPCR data.

Determination of STAT3 mRNA silencing (qRT-PCR analysis). For STAT3 expression, cells were transfected with 50 nM of Anti-STAT3 dsiRNA using dendrimer as described above. 48 h post-transfection, total RNAs were isolated and expression of the STAT3 coding RNAs was analyzed by qRT-PCR as previously described. . Primers were as follows: STAT3 forward Primer: 5’- GCA GGA GGG CAG TTT GAG -3’; STAT3 reserved Primer: 5’- CGC CTC AGT CGT ATC TTT CTG -3’; GAPDH forward primer: 5’- CAT TGA CCT CAA CTA CAT G-3’; GAPDH reverse primer: 5’- TCT CCA TGG TGG TGA AGA C-3’. GAPDH expression was used for normalization of the qPCR data. qRT-PCR reactions were amplified as described above.

In vivo gene silencing in tumor-xenografted nude mice: Institutional guidelines for the proper and human use of animals in research were followed. Approximately 10×10^6 PC-3 cells were inoculated subcutaneously with 0.1 mL of DMEM (Lonza) which was supplemented with 10% FBS in the flank region of 5-week-old male xenograft nude mice (Charles River Laboratories, Larbresles, France) *via* a 27-gauge needle. As previously described when PC-3 tumors reached 50 mm^3, usually 3 to 4 weeks after injection, mice were randomLy selected for treatment with Hsp27 siRNA/amphiphilic dendrimer **AD**, scrambled siRNA/amphiphilic dendrimer **AD**, Hsp27 siRNA alone, amphiphilic dendrimer **AD**, or PBS buffer alone. Each experimental group consisted of 5 mice. After randomization, PBS buffer, 3 mg/kg Hsp27 siRNA, amphiphilic dendrimer **AD** at N/P ratio of 5, Hsp27 siRNA/amphiphilic dendrimer **AD** or scrambled siRNA/amphiphilic dendrimer **AD** complexes were injected intraperitoneally twice per week for 5 week. The size of the tumors and the weight of mice were recorded once per week. After five weeks of treatments, mice were sacrificed, and tumors were removed from the animals. Tumors were frozen in liquid nitrogen and then stocked at -80 ℃ for RNA and protein extraction. The in vivo expression of Hsp27 mRNA and protein were measured, respectively, by qRT-PCR

and Western blot as described before.

In vivo toxicity evaluation in male C57BL/6 mice:

Institutional guidelines for the proper and human use of animals in research were followed. To assess the in vivo toxicity of dendrimer **AD** mediated siRNA delivery system, several important parameters were tested. Six-to-eight week-old male C57BL/6 mice with the weight of 18-22 g were randomly divided into 4 groups. Each experimental group consisted of 5 mice. After randomization, PBS buffer, 3 mg/kg of siRNA/amphiphilic dendrimer **AD** (N/P ratio 5), siRNA alone and amphiphilic dendrimer **AD** alone were injected once intravenously (i.v.). Three hours later, mice were sacrificed and serum specimens were collected. The three important hepatic indicators - AST (aspartate transaminase), ALT (alanine transaminase) and γ-GT (gamma glutamyl transaminase) were measured. Meanwhile the CHO (cholesterol) in serum and the two indicators of kidney function, BUN (blood urea nitrogen) and CRE (creatinine), were evaluated. All the detection was performed using SABA-18 Automatic Biochemical Analyzer (Analyzer Medical System, Roma, Italy).

H&E staining (hematoxylin-eosin staining)

In order to further assess the biocompatibility and biosafety of dendrimer, histochemistry and microstructure of main organs were investigated by microscopy. Briefly, mice were sacrificed by cervical dislocation 24 hours post administration. The main organs, including heart, liver, spleen and kidney, were fixed with 4% neutral formalin. Then specimens were dehydrated by graded alcohol solutions, followed by transparentizing with dimethylbenzene, embedding by paraffin, sectioning, dewaxing and staining according to the standard procedures. The final H&E stained sections were observed by using an inverted fluorescence microscope (Olympus X71, Olympus, Tokyo, Japan).

Statistical analysis

Statistical analysis was performed by Student's test (t-test) (Microsoft Excel 2003). $p \leqslant 0.05$ was considered significant (*); $p \leqslant 0.01$ (**); $p \leqslant 0.001$ (***).

Computational section

Scale integration in specific contexts in the field of (bio)molecular modeling can be done in different ways. Any recipe for passing information from one scale (usually lower) to another (higher) scale is based on the proper definition of many-scale modeling which considers objects that are relevant at that particular scale, disregards all degrees of freedom of smaller scales, and summarizes those degrees of freedom by some representative parameters. Specifically, the multiscale modeling strategy developed by our group[3],[4],[5],[6],[7] is based on the systematic elimination of computationally expensive degrees of freedom while retaining implicitly their influence on the remaining degrees freedom in the mesoscopic model. Accordingly, using the information obtained from atomistic molecular dynamics (MD) simulations we parameterized the coarse-grained (e.g., Dissipative Particle Dynamics (DPD)[8],[9]) models that incorporate all essential physics/phenomena observed at the finer level.

The outline of the general strategy of our multiscale modeling approach may be summarized as follows: first, explicit solvent atomistic MD calculations were performed on the **AD** model compound and its assembly with siRNA;[10],[11],[12],[13],[14] then, the mesoscale model parameters were calculated exploiting the conformational properties and energetical values obtained from MD simulation[15],[16],[17],[18],[19] using an explicit solvent model in which each **AD** dendron and siRNA segment were represented as single force centers (beads) and solvent was treated explicitly in the presence of ions and counterions. Langevin dynamics were then conducted using the DPD representation of the system.

Atomistic molecular dynamics (MD) simulations of 1:1 AD/siRNA complexes: All simulations and data analysis were performed with the AMBER 11 suite of programs.[20] The sequence of Hsp27 siRNA was employed to build the corresponding siRNA 3D model using the *Nucleic Acid Builder* (NAB) modulus implemented in *Amber Tools* 1.5.[20] Then, the **AD** model was built and optimized using the *Antechamber* module of AMBER 11 and the GAFF force field.[21]

The **AD** structure was then solvated in a TIP3P[22] water box, extending 20 Å from the

solute in the three dimensions, and a suitable number of Na^+ and Cl^- ions were added to neutralize the system and to mimic ionic strength, removing eventual overlapping water molecules. The solvated dendrons were subjected to a combination of steepest descent/conjugate gradient minimization of the potential energy, during which bad contacts between water and the compound were relieved. The relaxed systems were then gradually heated to 300 K in three intervals by running NVT MD simulation, allowing a 0.5 ns interval per each 100 K. Subsequently, 10 ns MD simulations under isobaric-isothermal (NPT) conditions were conducted to fully equilibrate the solvated **AD** system. From the corresponding equilibrated systems, all water molecules and counterions were removed, and the siRNA chain was placed in contact via its major groove with the **AD** molecule. The resulting structure was again solvated with a water box extending 30 Å from the solute. Counterions were then added in two steps: firstly, only the counterions necessary to ensure system neutrality were introduced while, in a further step, the proper amount of Na^+ and Cl^- ions was added.

The **AD**/siRNA assembly was initially relaxed by minimizing water bad contacts. This was achieved by running again a combined cycle of steepest descent/conjugate gradient potential energy minimization while fixing the **AD**/siRNA complex in its initial configuration using a harmonic constraint with a force constant of 500 kcal/(mol $Å^2$). Subsequently, the system was gradually heated to 310 K in three intervals, allowing a 1 ns interval per each 100 K, still using a weak 25 kcal/(mol $Å^2$) harmonic constraint on the complex in order to allow for its slow relaxation,[3],[4],[5],[6],[7],[10],[11],[12],[13],[14] The *Shake* algorithm[23] with a geometrical tolerance of 5×10^{-4} Å was imposed on all covalent bonds involving hydrogen atoms. 10 ns of NPT MD simulations were then run at 300 K to achieve full system equilibration. At this point, these MD runs were followed by other 10 ns NPT MD simulations during which the force constant of the harmonic constraints were gradually brought to zero in steps of 5 kcal/(mol $Å^2$) each. Finally, 40 ns of NVT MD data collection runs were carried. Temperature control was achieved using the Langevin[24] temperature equilibration scheme and an integration time step of 2 fs. The particle mesh Ewald method[25] was used to treat the long-range electrostatics.

For the calculation of the binding free energy between the siRNA and the **AD** molecule, 4000 snapshots were saved during the MD data collection period described above, one snapshot per each 10 ps of MD simulation.

All production MD simulations were carried out by using the *ff03* all-atom force field by Duan et al.[26] working in parallel on IBM FERMI and Eurora calculation cluster of the CINECA supercomputer centre (Bologna, Italy). The energetic analysis was performed by running the Molecular Mechanics/Poisson-Boltzmann Surface Area (MM/PBSA)[23],[27] script supplied with AMBER 11 on the last equilibrated 40 ns MD trajectory.

Dissipative Particle Dynamics (DPD) theory: DPD is a particle-based mesoscale technique first introduced by Hoogerbrugge and Koelman[9] and cast in its present form by Español and Warren, and Groot and Warren[8]. In DPD, a number of particles are coarse-grained into fluid elements, called beads. These DPD beads interact via pairwise additive interactions that locally conserve momentum, a necessary condition for a correct description of hydrodynamics, while retaining essential information about the structural and physical-chemical properties of the system components. An advantageous feature of DPD is that it employs soft repulsive interactions between the beads, thereby allowing for larger integration time steps than in a typical molecular dynamics using for example Lennard-Jones interactions. Thus, time and length scales much larger (up to microseconds range) than those in atomistic molecular dynamics simulations can be accessed.

There are three types of forces between dissipative particles. The first type is a conservative force ($\boldsymbol{F_{ij,C}}$) deriving from a soft potential that tries to capture the effects of the "pressure" between different particles. The second type of force is a friction force ($\boldsymbol{F_{ij,D}}$) between the particles that wants to describe the viscous resistance in a real fluid. This force tries to reduce velocity differences between dissipative particles. Finally, there is a stochastic force ($\boldsymbol{F_{ij,R}}$) that describes the degrees of freedom that have been eliminated from the description in the coarse-graining process. This stochastic force will be responsible for the Brownian motion of (macro)molecules and colloidal

particles simulated with DPD:

$$d\boldsymbol{r}_i(t) / dt = \boldsymbol{p}_i(t) / m_i \quad \text{(SI1)}$$

$$d\boldsymbol{p}_i(t) / dt = \boldsymbol{f}_i(t) \quad \text{(SI2)}$$

where $\boldsymbol{r}_i(t)$, $\boldsymbol{p}_i(t)$, m_i, and $\boldsymbol{f}_i(t)$ are the position, momentum, mass and net force of particle i, respectively. $\boldsymbol{f}_i(t)$ is given as the sum of three different forces: the conservative force $\boldsymbol{F}_{ij,C}$, the dissipative force $\boldsymbol{F}_{ij,D}$, and the random force $\boldsymbol{F}_{ij,R}$:

$$\boldsymbol{f}_i(t) = \Sigma_{i \neq j} \boldsymbol{F}_{ij,C} + \boldsymbol{F}_{ij,D} + \boldsymbol{F}_{ij,R} \quad \text{(SI3)}$$

All forces are pairwise and lay along the line joining two interacting particles i and j. The expressions for the forces are given by the following equations:

$$\boldsymbol{F}_{ij,C} = a_{ij} (1 - r_{ij} / r_c) \times \boldsymbol{r}_{ij} / r_{ij} \quad \text{(SI4)}$$

$$\boldsymbol{F}_{ij,D} = -\gamma_{ij} \omega^D(r_{ij}) [(\boldsymbol{r}_{ij} / r_{ij}) \times \boldsymbol{v}_{ij}] (\boldsymbol{r}_{ij} / r_{ij}) \quad \text{(SI5)}$$

$$\boldsymbol{F}_{ij,R} = \sigma_{ij} \omega^R(r_{ij}) (\zeta_{ij} / \Delta t^{0.5}) (\boldsymbol{r}_{ij} / r_{ij}) \quad \text{(SI6)}$$

where a_{ij} is the maximum repulsion parameter between particle i and j, $\boldsymbol{r}_{ij} = \boldsymbol{r}_i - \boldsymbol{r}_j$ is the vector joining beads i and j, $r_{ij} = |\boldsymbol{r}_{ij}|$ is the distance between particle i and j, $\boldsymbol{v}_{ij} = \boldsymbol{v}_i - \boldsymbol{v}_j$ is the relative velocity, and $\boldsymbol{v}_i = \boldsymbol{p}_i / \mathrm{m_i}$. All the above forces acts within the cut-off radius r_c, which basically constitutes the length scale of the entire system. γ_{ij} is a friction coefficient, σ_{ij} the noise amplitude, ζ_{ij} a Gaussian random number with a zero mean and a unit variance chosen independently for each pair of particles, and Δt is the time step in the simulation. $\omega^D(r_{ij})$ and $\omega^R(r_{ij})$ are weight functions vanishing for distance greater than r_c.

In DPD, molecules are built by tying beads together using Hookean springs with the potential given by:

$$U_{bb}(i, i+1) = \tfrac{1}{2} k_{bb} (r_{i,i+1} - l_0)^2 \quad \text{(SI7)}$$

where i, $i+1$ label adjacent beads in the molecule. The spring constant, k_{bb}, and unstretched length l_0, are chosen so as to fix the average bond length to a desired value. Chain stiffness is modeled by a three body potential acting between adjacent bead triples in a row using equation (SI8):

$$U_{bbb}(i\text{-}1,i,i\text{+}1) = k_{bbb}\,(1\text{-}\cos(\phi - \phi_0)) \qquad \text{(SI8)}$$

in which the angle ϕ is defined by the scalar product of the two bonds connecting the pair of adjacent beads *i-1*, *i*, and *i+1*.

DPD computational details

Comparing the appropriate MD and DPD pair-pair correlation functions, we determined the mesoscale topology of the **AD** molecule.[4],[16],[18],[19],[28] The coarse-grained model of the **AD** dendritic system so obtained is shown in Figure S13.

In detail, a neutral bead types C was identified as the hydrophobic chain building block. A neutral bead type R and a positively charged bead type RC were employed for the non-protonated and terminal charged repeating unit of the **AD** dendron, respectively. Two further bead type, G and L, the first linking the hydrophilic and hydrophobic parts together, and the second representing the dendron focal point, were also employed.

Solvent molecules were simulated by single bead types W, and an appropriate number of counterions of a charge of ± 1 were added to preserve charge neutrality and to account for the experimental solution ionic strength. The inclusion of explicit counterions was necessary because counterion condensation and the interactions between the counterions and the charged groups may affect the complex structure to a certain extent.

Following our previous work,[4],[5],[7] standard DPD particles were used to represent the siRNA chain beads, and the siRNA molecule was modeled as a self-avoiding string[29] of 24 DPD S particles which are sequentially connected through a WLC spring.[30] Moreover, in order to correctly derive the electrostatic interactions between charged beads, the electrostatic force between two charged beads *i* and *j* was analyzed following solving the electrostatic field by smearing the charges over a lattice grid, the size of which is determined by a balance between the fast implementation and the correct representation of the electrostatic field.[31]

Having set the reference volume of one bead and the density of the system to a value

of ρ=3, the appropriate number of **AD** and siRNA molecules were added to the simulation box in order to fit experimental concentrations and to reproduce an N/P ratio of 10. 7×10^6 time steps were performed in each DPD run, with a total physical time of each calculation being approximately 3s, to obtain the self-assembled morphology of the dendron alone and in presence of siRNA.

The intra- and intermolecular interactions between DPD particles are expressed by the conservative parameter a_{ij}, defined by equation (SI4). This quantity accounts for the underlying chemistry of the system considered. In this work, we employed a well-validated strategy that correlates the interaction energies estimated from atomistic molecular dynamics (MD) simulations to the mesoscale a_{ij} parameter values. [15],[16],[17],[18],[19]

Following this computational recipe, the interaction energies between the solvated 1:1 **AD**/siRNA systems estimated using the MM/PBSA[23],[27] methodology were rescaled onto the corresponding mesoscale segments adapting the procedure described in detail in references [18] and [19]. The bead-bead interaction parameter for water was set equal to a_{ww} = 25 in agreement with the correct value of DPD density ρ=3.[8] The maximum level of hydrophobic/hydrophilic repulsion was captured by setting the interaction parameter a_{ij} between the water bead W and the hydrocarbon tail bead C as 82. The counterions were set to have the interaction parameters of water.[32] Once these parameters were assigned, all the remaining bead-bead interaction parameters for the DPD simulations were easily obtained, starting from the atomistic interaction energies values. The entire set of DPD interaction parameters employed in this work are summarized in Table S1.

References

[1] T. Yu, X. Liu, A.-L. Bolcato-Bellemin, Y. Wang, C. Liu, P. Erbacher, F. Qu, P. Rocchi, J.-P. Behr, L. Peng, *Angew. Chem. Int. Ed.* **2012**, *51*, 8478-8484.

[2] X.-x. Liu, P. Rocchi, F.-q. Qu, S.-q. Zheng, Z.-c. Liang, M. Gleave, J. Iovanna, L. Peng, *Chem. Med. Chem.* **2009**, *4*, 1302-1310.

[3] P. Posocco, E. Laurini, V. Dal Col, D. Marson, K. Karatasos, M. Fermeglia, S. Pricl, *Curr. Med. Chem.* **2012**, *19*, 5062-5087.

[4] X. Liu, J. Wu, M. Yammine, J. Zhou, P. Posocco, S. Viel, C. Liu, F. Ziarelli, M. Fermeglia, S. Pricl, G. Victorero, C. Nguyen, P. Erbacher, J.-P. Behr, L. Peng, *Bioconjugate Chem.* **2011**, *22*, 2461-2473.

[5] A. Barnard, P. Posocco, S. Pricl, M. Calderon, R. Haag, M. E. Hwang, V. W. Shum, D. W. Pack, D. K. Smith, *J. Am. Chem. Soc.* **2011**, *133*, 20288-20300.

[6] S. P. Jones, N. P. Gabrielson, C.-H. Wong, H.-F. Chow, D. W. Pack, P. Posocco, M. Fermeglia, S. Pricl, D. K. Smith, *Mol. Pharm.* **2011**, *8*, 416-429.

[7] P. Posocco, S. Pricl, S. Jones, A. Barnard, D. K. Smith, *Chem. Sci.* **2010**, *1*, 393-404.

[8] R. D. Groot, P. B. Warren, *J. Chem. Phys.* **1997**, *107*, 4423-4435.

[9] P. J. Hoogerbrugge, J. M. V. A. Koelman, *Europhys. Lett.* **1992**, *19*, 155-160.

[10] X. Liu, C. Liu, E. Laurini, P. Posocco, S. Pricl, F. Qu, P. Rocchi, L. Peng, *Mol. Pharm.* **2012**, *9*, 470-481.

[11] K. Karatasos, P. Posocco, E. Laurini, S. Pricl, *Macromol. Biosci.* **2012**, *12*, 225-240.

[12] G. M. Pavan, P. Posocco, A. Tagliabue, M. Maly, A. Malek, A. Danani, E. Ragg, C. V. Catapano, S. Pricl, *Chem. Eur. J.* **2010**, *16*, 7781-7795.

[13] S. P. Jones, G. M. Pavan, A. Danani, S. Pricl, D. K. Smith, *Chem. Eur. J.* **2010**, *16*, 4519-4532.

[14] G. M. Pavan, A. Danani, S. Pricl, D. K. Smith, *J. Am. Chem. Soc.* **2009**, *131*, 9686-9694.

[15] P. Posocco, C. Gentilini, S. Bidoggia, A. Pace, P. Franchi, M. Lucarini, M. Fermeglia, S. Pricl, L. Pasquato, *ACS Nano* **2012**, *6*, 7243-7253.

[16] R. Toth, F. Santese, S. P. Pereira, D. R. Nieto, S. Pricl, M. Fermeglia, P. Posocco, *J. Mater. Chem.* **2012**, *22*, 5398-5409.

[17] P. Posocco, Z. Posel, M. Fermeglia, M. Lísal, S. Pricl, *J. Mater. Chem.* **2010**, *20*, 10511–10520.

[18] G. Scocchi, P. Posocco, J.-W. Handgraaf, J. G. E. M. Fraaije, M. Fermeglia, S. Pricl, *Chem. Eur. J.* **2009**, *15*, 7586-7592.

[19] G. Scocchi, P. Posocco, M. Fermeglia, S. Pricl, *J. Phys. Chem. B* **2007**, *111*, 2143-2151.

[20] D. A. Case, T. A. Darden, T. E. I. Cheatham, C. L. Simmerling, J. Wang , R. E. Duke, R. Luo, R. C. Walker, W. Zhang, K. M. Merz, B. Roberts, B. Wang, S. Hayik, A. Roitberg, G. Seabra, I. Kolossváry, K. F. Wong, F. Paesani, J. Vanicek, X. Wu, S. R. Brozell, T. Steinbrecher, H. Gohlke, Q. Cai, X. Ye, J. Wang, M.-J. Hsieh, G. Cui, D. R. Roe, D. H. Mathews, M. G. Seetin, C. Sagui, V. Babin, T. Luchko, S. Gusarov, A. Kovalenko, P. A. Kollman, in *AMBER 11*, University of California, San Francisco, CA, USA, **2010**.

[21] J. M. Wang, R. M. Wolf, J. W. Caldwell, P. A. Kollman, D. A. Case, *J. Comput. Chem.* **2004**, *25*, 1157-1174.

[22] J.-P. Ryckaert, G. Ciccotti, H. J. C. Berendsen, *J. Comput. Phys.* **1977**, *23*, 327-341.

[23] J. Srinivasan, T. E. Cheatham, P. Cieplak, P. A. Kollman, D. A. Case, *J. Am. Chem. Soc.* **1998**,

120, 9401-9409.

[24] R. J. Loncharich, B. R. Brooks, R. W. Pastor, *Biopolymers* **1992**, *32*, 523-535.

[25] M. K. Gilson, K. A. Sharp, B. H. Honig, *J. Comput. Chem.* **1988**, *9*, 327-335.

[26] Y. Duan, C. Wu, S. Chowdhury, M. C. Lee, G. Xiong, W. Zhang, R. Yang, P. Cieplak, R. Luo, T. Lee, J. Caldwell, J. Wang, P. Kollman, *J. Comput. Chem.* **2003**, *24*, 1999-2012.

[27] P. Posocco, M. Fermeglia, S. Pricl, *J. Mater. Chem.* **2010**, *20*, 7742-7753.

[28] S. M. Bromfield, A. Barnard, P. Posocco, M. Fermeglia, S. Pricl, D. K. Smith, *J. Am. Chem. Soc.* **2013**, *135*, 2911-2914.

[29] V. Symeonidis, G. Em Karniadakis, B. Caswell, *Phys. Rev. Lett.* **2005**, *95*.

[30] E. Moeendarbary, T. Y. Ng, H. Pan, K. Y. Lam, *Microfluid. Nanofluid.* **2010**, *8*, 243-254.

[31] R. D. Groot, *J. Chem. Phys.* **2003**, *118*, 11265-11277.

[32] X. Fan, N. , S. Phan-Thien, X. W. Chen, T. Y. Ng, *Phys. Fluids* **2006**, *18*, 63102–63110.